

# Experimental and Theoretical Study of Symmetric Dimeric Oligomers

Hunter Johnson

Supervisors: Dr. Gerry Marangoni, and Dr. M. Shajahan Razul

Thesis submitted in partial fulfillment of the  
the requirements for the degree of  
Bachelor of Science with Honours in Chemistry

*Saint Francis Xavier University*

*Antigonish, N.S.*

*March 2026*

© Copyright Hunter Johnson 2026

Saint Francis Xavier University

Department of Chemistry

The undersigned hereby certify that they have read the thesis entitled “**Experimental and Theoretical Study of Symmetric Dimeric Oligomers**” by Hunter Johnson in partial fulfillment of the requirements for the degree **Bachelor of Science with Honours**

Date: \_\_\_\_\_

Supervisor: \_\_\_\_\_

Saint Francis Xavier University

May 2026

Author: Hunter Johnson

Title: **Experimental and Theoretical Study of Symmetric Dimeric Oligomers**

Department: Chemistry

Faculty: Science

Convocation: May 2026

Permission is herewith granted to Saint Francis Xavier University to circulate and to have copied for non-commercial purposes, at its discretion, the above title upon request of individuals or institutions.

---

Hunter Johnson

The author reserves other publication rights, and neither the thesis nor extensive extractions from it may be printed or otherwise reproduced without the author's written permission.

The author attests that permissions have been obtained for the use of any copyrighted material appearing in this thesis (other than a brief excerpt requiring only proper acknowledgement in scholarly writing) and that all such use is clearly acknowledged.

## ***Table of Contents***

Abstract .....	vii
List of Figures .....	viii
List of Tables.....	x
List of Abbreviations.....	xi
Acknowledgements .....	xiii
1. Introduction.....	1
1.1. Overview .....	1
1.2. Computational Background .....	2
1.3. Thesis .....	3
2. Surfactant Theory.....	5
2.1. Surface Active Agents and Their Aggregate Forms.....	5
2.2. Fundamental Properties of Micelles .....	9
2.3. Mixed Micelles.....	10
2.4. The Mixed Micelle and Gemini Surfactant Problem .....	11
3. Computational Theory.....	13
3.1. Computational Chemistry.....	13
3.2. Computational Studies of Micellar Structures .....	15
3.3. Radial Distribution Functions .....	16
4. Materials and Methods.....	19
4.1. Computational .....	19
4.1.1. The Model.....	19
4.1.2. Simulation Radial Distribution Functions .....	21
4.1.3. Comparative Energetics Experiments.....	23
5. Results and Discussion .....	24
5.1. Non-Mixed Surfactant System to 2D <sup>1</sup> H-NMR Experiments .....	24
5.2. Mixed Surfactant System to a Non-mixed System.....	31
5.3. System Size Effects on a Mixed System of 10-4-10:10-6-10 .....	34
5.4. Energetics Comparison of 10-4-10:10-6-10.....	38
6. Conclusions and Future Work.....	40
6.1. Conclusions .....	40

6.2. Future Work.....41

7. REFERENCES.....43

## Abstract

Although multiple families of gemini surfactants have been studied in the literature. Meaningful structure performance relationships are limited to a single family. As such building a model to readily study dimeric surfactants may provide a means for structural performance evaluations of experimentally synthesized surfactants and their computationally generated counterparts.

The bending of the interchange arm of gemini or dimeric surfactants has been studied in a dynamic computational model. Conformational behaviour of the surfactants in simulation have been assessed via radial distribution functions or “RDFs”. The results indicate the longer spacers can loop towards the aggregate interior and interact with the protons on the carbon atoms near the end of the main surfactant chains, whereas these interactions are absent for the shortest spacer dimeric studied. These conformational patterns suggested from the RDF results have been compared to experimentally determined conformations and orientation of a series of dicationic dimeric amphiphiles of the type N,N'-bis (dimethylalkyl)- $\alpha,\omega$ -alkanediammonium dibromide (*m-s-m*) in aggregated form via  $^{13}\text{C}$  chemical shift measurements and 2D-rotating frame Overhauser enhancement spectroscopy (2D-ROESY). Using the non-mixed systems as a reference point, the conformational behaviour of mixed systems of surfactants has been contrasted.

## List of Figures

Figure 2-1 - Depiction of a typical surfactant.....	5
Figure 2-2 - A simple cross-sectional display of a spherical micelle.....	6
Figure 2-3 - Schematic of different aggregation types. (From Poolakkandy et al. 2020).....	7
Figure 2-4 - Optimized (DFT b3lyp/6-31+g(d)) depiction of a 10-4-10 gemini surfactant built using the Gaussian software. Hydrogen atoms are hidden for clarity. ....	9
Figure 2-5 - Cross section of a mixed micelle, the blue tail represents an alkyl chain of length $m$ , while the orange tail represents an alkyl chain of length $n$ . ....	11
Figure 2-6 - Proposed mechanisms of mixed micelle formations, the orange tail denotes an alkyl chain of length $m$ , the blue head represents the two nitrogen heads connected by a spacer length $s$ , and the green head represents the two nitrogen heads connected by a spacer length $z$ . ....	12
Figure 3-1 - A simple system depicting periodic boundary conditions, the object in the center box as well as its motion is reflected periodically outwards in all directions to alleviate the effects of a hard boundary. ....	14
Figure 3-2 - Depiction of forcefield parameters considered in molecular dynamics (Pink et al.)	15
Figure 3-3 - Schematic showcasing the theory behind Radial Distribution Functions. ....	17
Figure 3-4 - oxygen-oxygen radial distribution function of SPCE water at 298K. The dotted, solid, and dashed lines correspond to the classical, quantum $H_2O$ , and quantum $D_2O$ results. (Hernández et al.) ....	17
Figure 4-1 - Block diagram of the preparation stages of the proposed model.....	20
Figure 4-2 - A numerical description of a 10-10-10 dimeric. Spacer chain carbons are counted from $N1$ and given the tag $S$ , alkyl chain carbons are counted from their attached Nitrogen head and given the tag $A$ for those attached to $N1$ , and $A'$ for those attached to $N2$ . ....	22
Figure 5-1 - Radial distribution function of 2S-4A. The blue line represents the 2-length spacer chain, orange represents $s = 4$ , green represents $s = 6$ , turquoise represents $s = 8$ , and purple represents $s = 10$ . ....	25
Figure 5-2 - An RDF of 1S-1A and (B) the RDF for [1S-1A]. The blue line represents $s = 2$ , orange represents $s = 4$ , green represents $s = 6$ , turquoise represents $s = 8$ , and purple represents $s = 10$ . ....	26
Figure 5-3 - Radial distribution function of 10A-10A'. The blue line represents the 2-length spacer chain, orange represents $s = 4$ , green represents $s = 6$ , turquoise represents $s = 8$ , and purple represents $s = 10$ . ....	27
Figure 5-4 - Radial distribution function of 2S-4A. The blue line represents the 2-length spacer chain, orange represents $s = 4$ , green represents $s = 6$ , turquoise represents $s = 8$ , and purple represents $s = 10$ . ....	28
Figure 5-5 - (A) RDF corresponding to 1S-10A. The blue line represents the 2-length spacer chain, orange represents $s = 4$ , green represents $s = 6$ , turquoise represents $s = 8$ , and purple represents $s = 10$ . (B) 1S-1A RDF of 10-6-10 that has had its inter and intramolecular interactions decoupled. The blue line represents [1S-10A], while the orange line represents [1S-10A). ....	30
Figure 5-6 - Proposed aggregation scheme of a random dispersion of 10-10-10 (A) into a typical aggregation (B) and a semi aggregate (C). The model serves to provide a reasoning for the appearance of terminal carbons within a shorter distance than the intramolecular distance denoted by the arrows. ....	30

<i>Figure 5-7 - (A) 1S-10A RDF of 10-2-10 in solution with a secondary surfactant. The blue line represents a 10-2-10 in solution with 10-10-10, orange represents a mix with 10-4-10, green represents a mix with 10-6-10, turquoise represents a mix with 10--8-10, and purple represents the unmixed 10-2-10. (B) 1S-10A RDF of 10-6-10 in solution with a secondary surfactant. Three simulations shown to highlight difference, dark blue represents a mix with 10-10-10, the orange represents a mix with 10-8-10, and the green represents the unmixed 10-6-10.....</i>	<i>32</i>
<i>Figure 5-8 - 10A-10A' RDF of 10-6-10 in a mixed solution. The blue line represents a mix with 10-10-10, the orange line represents a mix with 10-8-10, and the green line represents an unmixed 10-6-10 solution. ....</i>	<i>32</i>
<i>Figure 5-9 - (A) 2S-3A RDF of 10-4-10, the turquoise line is the unmixed solution. (B) 2S-3A RDF of 10-6-10 the green line represents the unmixed 10-6-10, and (C) 2S-3A RDF of 10-2-10, the purple line represents the unmixed 10-2-10. ....</i>	<i>33</i>
<i>Figure 5-10 - (A) 1S-1A RDF of 10-4-10 in a mixed system with 10-6-10 (B) 1S-1A RDF of 10-6-10 in a mixed system with 10-4-10. The blue line is the 40:40 while the orange is the 5:5 system. ....</i>	<i>35</i>
<i>Figure 5-11 - Figure 5-11: 2S-3A of a 10-4-10 (A) and a 10-6-10 (B). The blue line represents a system size 40:40, and the orange line represents a system size 5:5.....</i>	<i>37</i>
<i>Figure 5-12 - A 10-6-10 RDF of 1S-10A in a mixed solution with 10-4-10. The blue line represents the 40:40, while the orange represents 5:5.....</i>	<i>38</i>
<i>Figure 5-13 - Potential energy of a 10-4-10:10-6-10 system as a function of surfactant count. .</i>	<i>39</i>

## List of Tables

Table 1 – Surfactant systems investigated in the present thesis with the number of water molecules used in the simulations.....	19
---	----

## List of Abbreviations

<b>LJ</b>	<b>Lennard-Jones</b>
<b><sup>1</sup>HNMR</b>	<b>Hydrogen Nuclear Magnetic Resonance</b>
<b>1S-10A</b>	<b>Alpha spacer to omega alkyl chain</b>
<b>1S-1A</b>	<b>Alpha spacer to alpha alkyl chain</b>
<b>2D-<sup>1</sup>HNMR</b>	<b>Two-Dimensional Hydrogen Nuclear Magnetic Resonance</b>
<b>2D-ROESY</b>	<b>Two-Dimensional Rotating-frame Overhauser Enhancement Spectroscopy</b>
<b>2S-3A</b>	<b>Beta spacer to gamma alkyl chain</b>
<b>2S-4A</b>	<b>Beta spacer to delta alkyl chain</b>
<b>CMC</b>	<b>Critical micelle concentration</b>
<b>CPB</b>	<b>cetylpyridium bromide</b>
<b>DFT</b>	<b>Density Functional Theory</b>
<b>GROMACS</b>	<b>Groningen Machine for Chemical Simulations</b>
<b>GROMOS</b>	<b>Groningen Molecular Simulation</b>
<b>ITC</b>	<b>Isothermal Titration Calorimetry</b>
<b>MC</b>	<b>Monte-Carlo</b>
<b>MD</b>	<b>Molecular Dynamics</b>
<b>NOESY</b>	<b>Nuclear Overhauser Effect Spectroscopy</b>
<b>NPT</b>	<b>Particles Pressure and Temperature</b>
<b>NVT</b>	<b>Particles Volume and Temperature</b>
<b>RDF</b>	<b>Radial Distribution Function</b>
<b>ROESY</b>	<b>Rotating-frame Overhauser Enhancement Spectroscopy</b>

<b>SPC</b>	<b>Simple Point Charge</b>
<b>SPCE</b>	<b>Extended Simple Point Charge</b>
<b>StFX</b>	<b>Saint Francis Xavier</b>
<b>TC</b>	<b>Terminal Carbon</b>
<b>USA</b>	<b>United States of America</b>
<b>USD</b>	<b>United States Dollar</b>

## Acknowledgements

Firstly, I would like to thank my two supervisors on this project, Dr. Marangoni and Dr. Razul. Any questions I had about the software were always readily answered by Dr. Razul, and he balanced out my stress on the project, being as relaxed as he is I might not have finished the project without that balance. Of course I must extend this gratitude to Dr. Marangoni as well, the door to his office was always open whenever I had a question regarding the physical chemistry side of things, and aside from that you were always available to chat about anything that was on my mind. Both were indispensable during this project, and I couldn't have asked for a better pair.

I would like to acknowledge further, the the entire chem department. This project wouldn't have come together without such an amazing community of people, students and staff. With that said there are four names that shaped my career at StFX: Dr. Aquino, for initially pushing me to do an honours, seeing the amount of Chem I wanted to take, I can see why you told me to "reach for the stars" and I'm glad I did. Dr. Foo, thank you for giving me a foray into the research side of chemistry. Dr. Orlova and Chem 421, seeing a different side of chemistry this late into the game really sparked an interest in pursuing a computational project. Finally, I would like to thank Dr. MacLean for encouraging me to stick with the Honours program when I really didn't want to, the grass really is greener on the other side.

Lastly, I would like to thank my family friends, and community for their support throughout my degree. To my closest friend John, thank you for listening to my advice and pursuing a degree at StFX, you have made my time here that much more enjoyable, and I hope your own endeavors are all as enjoyable as this was. Of course, I must thank Noah Russica for all your help during my degree as well. I will never forget our study sessions before Analytical Chem, drinking a few coffee pots between the two of us, and coming to the test severely sleep deprived.

I must extend gratitude to my community Potlotek First Nation. This community has provided me with opportunities not readily available to all people. I am glad I didn't waste the opportunity, and I hope to continue to show you what your continued support has wrought. And to my parents, thank you for all your support, this accomplishment truly would not have been possible without your support.

# 1. Introduction

## 1.1. Overview

Surfactants are found in many aspects of our daily lives; consequently this is the focus of a significant amount of research activity both industrially and in academia.<sup>1-3</sup> Surfactants have the ability, due to the nature of the molecule (that being a molecule with a polar headgroup and nonpolar, typically alkyl chains *Figure 2-1*), to “self-assemble” into structures called micelles, see *Figure 2-2*. The term, “micelle” was first coined by James W. McBain and colleagues in the early 20<sup>th</sup> century.<sup>4</sup> A typical micelle in aqueous medium will have their polar heads facing outwards maintaining contact with the aqueous medium, and their nonpolar tails facing the interior of the micelle. Surfactants have a host of applications based on their ability to self-assemble into micelles. This property is important in detergency, medicine and pharmacology (drug delivery), soil remediation, and a variety of other commercial applications since these micellar assemblies can incorporate water insoluble molecules in their interiors, a process known as solubilization. This means that materials normally not soluble in an aqueous environment can be made soluble; this is one of many useful properties of surfactants that has allowed their industrial usage to explode over the past 40 years.<sup>5,6</sup>

The global surfactant market had a net worth of USD 49.71 billion in 2025, with expectations to rise upwards to USD 77.25 billion annually by 2034.<sup>49</sup> With this perpetually growing market, improvements to surfactant applications for various uses will inevitably follow. The growth and innovation in surfactant-based technologies have led to the emergence and study of surfactants of varying chemical structures. Gemini (or dimeric) surfactants represent one of the most interesting and active areas of surfactant synthesis and research that have emerged in

surfactant chemistry in many years.<sup>1,7</sup> This thesis will use computational chemistry to examine the packing of the surfactant monomers in the self-assembled aggregates of a well-studied gemini surfactant, the dicationic gemini surfactants, that are based on quaternized, long-chain alkylamines. Chapter 1 will provide some background on the relevant information in the thesis. Chapter 2 will examine the properties of surfactants and self-assembled systems. Chapter 3 will discuss the theory behind the computational methods used in this thesis. In Chapter 4, the materials and methods used in the present thesis will be described. In Chapter 5, the computational results will be presented and discussed, and finally Chapter 6 will present some conclusions and offer some ideas for future work related to this thesis.

## 1.2. Computational Background

Computational theoretical chemistry is a subfield of chemistry that uses mathematical methods and fundamental laws of physics in studying chemical processes. The models describe molecules as a collection of atoms that have various charged components (positive nuclei, and negative electrons). In theoretical chemistry an important consideration for developing the models are the coulomb interaction terms, and how these interactions differ with respect to their coordinates. For the longest time, the only solvable systems theoretical chemistry could solve were systems consisting of one or two bodies that can be converted into a one body problem with the introduction of a center of mass. However analytical approaches such as perturbation theory have been proposed to solve (or approximate) n-body problems.<sup>8</sup>

The term *computational theoretical chemistry* may suggest supercomputers performing tasks the likes of which humans cannot comprehend but this is far from the case. Computers in fact are not as sophisticated as they appear, at their core they perform only the following:

mathematical operations, determine relationships between numbers, branching depending on a decision, looping, and reading data and the writing of said data to external files. The real genius of computers lies in their speed, and it is this speed that when paired with a good computational model allows theoretical chemistry its success as a predictive tool. This thesis will use computational chemistry to examine the packing of the amphiphile chains and the spacers linking the headgroups of some dicationic gemini surfactants as a function of the spacer length ( $s$ ) at a constant alkyl chain length ( $m = 10$ ). It is anticipated that the packing of the amphiphiles in the micelles will be impacted by the length of the spacer group; this will be probed computationally through the use of the radial distribution functions obtained from our simulations, and by comparison of the correlation functions for the carbon atoms of these amphiphiles to the results for the cross-peaks observed in the  $^1\text{H}$  and  $^{13}\text{C}$  shifts for these same gemini amphiphiles recently accepted for publication from this lab.

### 1.3. Thesis

Gemini (or dimeric) surfactants present an interesting variation on surfactants in that there are two head groups connected by a spacer.<sup>7</sup> Gemini surfactants pose a test of current micellization theories as it is anticipated that the rich diversity of structures should have a strong influence on the micellization process and of course, the thermochemical properties of the micelles they form.<sup>1,9,10</sup> Although multiple families of symmetric gemini surfactants have been studied in the literature,<sup>11</sup> structure performance relationships afforded by the complexity of the surfactant architecture (e.g., by varying the ratio of the main surfactant chains at constant spacer length or having two dissimilar head groups), are limited mainly to a single family, most likely due to the difficult nature of the gemini surfactants syntheses reported in the literature (i.e., low yields,

resource intensive, and time consuming).<sup>9</sup> Although there are multiple families of dimeric surfactants reported in the literature, the lack of monomeric or even dimeric amphiphiles with which a meaningful comparison can be made means that structure performance relationships and even details such as how the monomers and the spacers can efficiently pack into aggregates is lacking. Indeed, for many families of gemini surfactants, the absence of a monomeric counterpart makes meaningful structure performance comparisons impossible. As such, building a model to readily study dimeric surfactants will prove useful in not only obtaining information about these dimers without the issues outlined above, it may also provide a means for structural performance evaluations of experimentally synthesized dimeric surfactants against their computationally generated monomeric counterparts. For this thesis, the surfactants chosen are members of the N,N'-bis(dimethylalkyl)- $\alpha$ - $\omega$ -alkanediammonium dibromide family, with the counterion modified to chloride anions. Their dimeric form will be referred to by a shorthand nomenclature *m-s-m* where *m* is the length of the alkyl tail and *s* is the length of the alkyl spacer chain. These systems have been chosen as they are the most-studied dimeric surfactant family in the literature, and as such there exists a reasonable knowledge base for both these surfactants and their monomeric analogues with which meaningful comparisons and insights from our computational model can be obtained.

## 2. Surfactant Theory

### 2.1. Surface Active Agents and Their Aggregate Forms

Surface active agents (commonly known by the acronym surfactants), are well known for their activity at interfaces. This property of surfactants is attributed to their regions of differing polarity in the molecule, that being a region of hydrophobicity as a consequence of the alkyl chain, and a region of hydrophilicity due to the polar head. The efficiency of a surfactant is assessed by its ability to reduce the surface tension at the interface. An effective surfactant has the ability to reduce the surface tension of water from  $72\text{mNm}^{-1}$  to  $30\text{mNm}^{-1}$ .<sup>12</sup> There are classes of surfactants such as multi-tailed, multiheaded, gemini and of course the 4 main categories under which all surfactants can be classed (anionic, cationic, non-ionic, and zwitterionic, based on the charges of the surfactant headgroups). Surfactants are typically petroleum based in nature, but there are others, namely biosurfactants, that are derived from natural sources.<sup>12</sup>

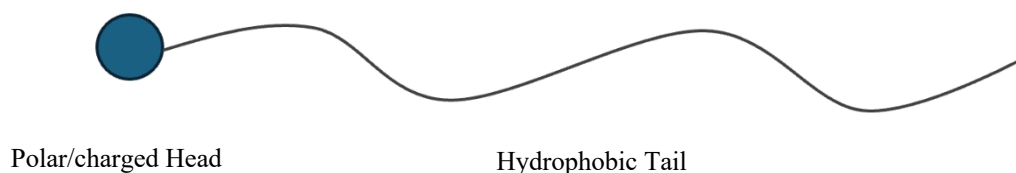


*Figure 2-1 - Depiction of a typical surfactant*

The most general surfactant depicted in *Figure 2-1* consists of a single alkyl chain (tail) connected to single polar or charged group (head). Further noted from *Figure 2-1*, the chain is not depicted as rigid, owing to the fact that alkyl bonds have a high degree of rotational freedom. This degree of freedom will be contextualized in chapter 5. The intermolecular and intramolecular interactions of the tails are considered to be indistinguishable from one another, as the micelle core

is described as “liquid-like” by David Gruen.<sup>13</sup> In having regions of both hydrophobicity and hydrophilicity, the molecule, when introduced to a polar solvent such as water will tend to aggregate into a structure called a micelle.<sup>14</sup> The most generic micelle is depicted in *Figure 2-2*, where we observe a cross section of a spherical micelle where the hydrophilic heads orient themselves outwards and the tails are pointed towards the interior of the aggregate. The solvent interaction with the molecule will result in an ordering of the water around the alkyl tails called the iceberg effect.<sup>15</sup> This is an entropically unfavoured process, although the clustering of the icebergs causes them to dissolve due to the strong cohesive effects of water. These cohesive effects will force the water back into the bulk solution, effectively “melting” the icebergs and allowing the alkyl chains to cluster, minimizing the nonpolar-polar interactions while increasing the entropy of the system. It is this effect (termed the “hydrophobic effect”) that causes spontaneous micellization above a certain concentration of surfactant known as the CMC (see **Section 2.2**).

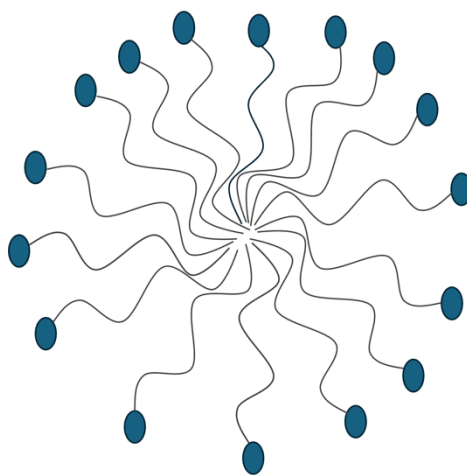


*Figure 2-2 - A simple cross-sectional display of a spherical micelle*

The type of aggregates that form in solution may be influenced by temperature, pH, and pressure of the system but it is predominantly due to the concentration and the structure of the

amphiphiles themselves.<sup>16</sup> A few of the many possible types of surfactants aggregates are represented in *Figure 2-3*. This aggregation is driven by the decrease in Gibbs energy due to the “melting” of icebergs defined by equation 2-1 below.

$$\Delta G = \Delta H - T\Delta S \quad [2-1]$$

The system after reaching a critical point, will allow the “icebergs” to cluster, and when in close enough proximity to melt, this will drive the equilibrium to a system of free surfactants with the various aggregates morphologies depicted below.

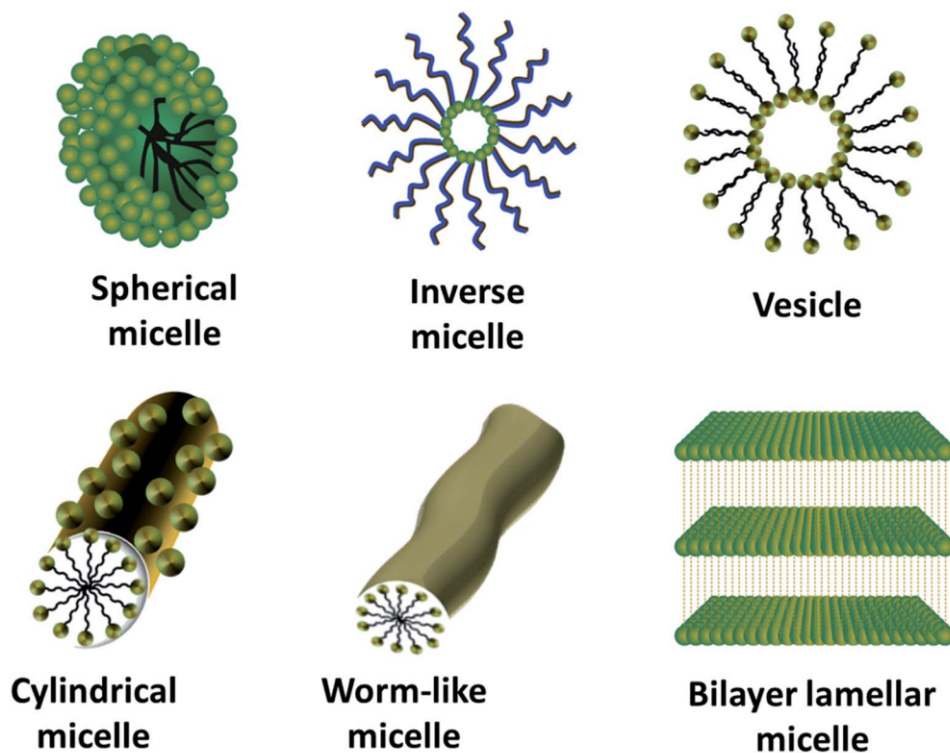


*Figure 2-3 - Schematic of different aggregation types. (From Poolakkandy et al. 2020).*

17

The structural aggregates outlined in *Figure 2-3* show the range of surfactant aggregates that can be produced. Types of these aggregates and their equilibria with surfactant monomers

have been extensively studied for single-headed-single tailed surfactants like those depicted in *Figure 2-1*. These aggregates and the equilibria established with other families of surfactants is an active area of investigation.

Gemini surfactants are a class of surfactant first described by Menger and Littau in 1991, emerging from a study of quaternary ammonium salts and their phosphate derivatives.<sup>9</sup> Interestingly, in that same study they allude to the fact that micelles of these gemini surfactants would form at lower concentration versus their monomeric counterparts, despite the fact they did not present any experimental data to verify this statement. Gemini surfactants as depicted in *Figure 2-4* consist of two alkyl tails, and two polar head groups which are connected via an alkyl spacer group. It is of course the presence of two alkyl chains as well as the spacer itself that drive micelle formation at a lower concentration due to the hydrophobic effects with water. As mentioned above, these surfactants are less studied compared to conventional single-headed surfactants; the main reason for this is the difficulty of their synthesis and lack of comparative studies. However, with recent increased usage of new techniques (e.g., microwave synthesis both for asymmetric and symmetric amphiphile molecules<sup>18,19</sup>), it is expected that both the availability and the complexity of dimeric surfactants will increase.

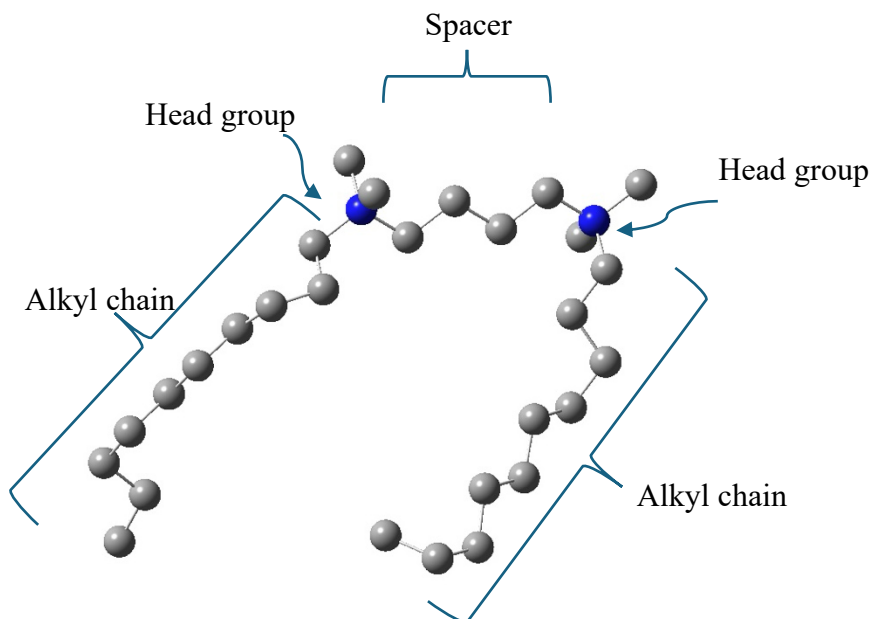


Figure 2-4 - Optimized (DFT b3lyp/6-31+g(d)) depiction of a 10-<sup>20, 44</sup>4-10 gemini surfactant built using the GaussView. Hydrogen atoms are hidden for clarity.

## 2.2. Fundamental Properties of Micelles

The critical point at which the “icebergs” melt and aggregates form is termed the critical micelle concentration (CMC). Below this value, surfactants are predominantly at the interface and the equilibrium between the monomers dissolved in the bulk of the solution and adsorbed at the interface can be modelled by a dynamic equilibrium. Above this value however, molecules begin to aggregate in the bulk phase, and any model of micelle formation must account for the significant decrease in the Gibbs energy that results when the surfactant molecules cooperatively self-assemble into micelles. The underlying thermodynamics governing the type of aggregate formed must take into account the shape and size of said aggregate.<sup>46</sup> The Krafft temperature,  $T_k$ , is the temperature at which the equilibrium between the self-assembled aggregates and the monomers

micelles begins to form in a saturated solution; below the Krafft temperature, the equilibrium is between solid, hydrated surfactant and dissolved monomers only. Another important property of surfactant micelles is the aggregation number, which is the average number of monomers comprising the micelles. Aggregation numbers depend on both the length of the alkyl chain of the surfactant and its concentration in solution above the CMC;<sup>21, 17</sup> typical values for aggregation numbers are between 50-100 surfactant molecules, although these numbers are large in higher order aggregates like worm-like micelles.<sup>3</sup>

### 2.3. Mixed Micelles

Recently, research focus has shifted to the study of mixed surfactant systems. A mixed system consists of multiple components of surfactants that often exhibit properties different from what would be expected of the individual surfactant types. One of the most interesting phenomena with respect to mixed micelles is the appearance of micelles at a lower concentration than their non-mixed counterparts, i.e. the CMC has effectively been lowered.<sup>22</sup> John H. Clint has done research on the micellization of mixed non-ionic surfactants in the 1970s, his experiments yielded an equation that can be used to predict the CMC in a system that is ideally mixed and is given by equation [2-2]:<sup>23</sup>

$$\frac{1}{CMC_{mix}} = \sum_i \frac{\alpha_i}{CMC_i} \quad [2-2]$$

For a two-component system:

$$\frac{1}{CMC_{mix}} = \frac{\alpha}{CMC_a} + \frac{1-\alpha}{CMC_b} \quad [2-3]$$

Where  $CMC_a$  is the critical micelle concentration of the first surfactant,  $CMC_b$  is the critical micelle concentration of the second surfactant,  $CMC_{mix}$  is the critical micelle concentration of the mixed micelles, and  $\alpha$  is the fraction of surfactant a in the system.

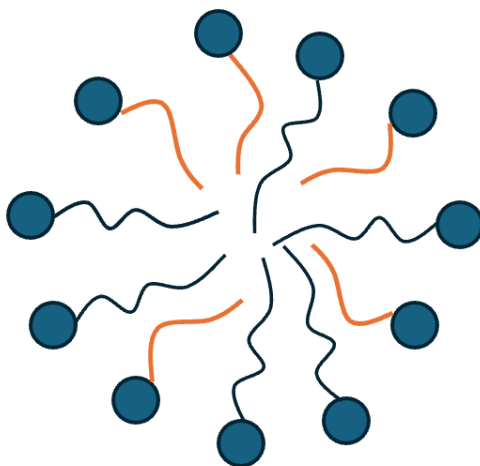


*Figure 2-5 - Cross section of a mixed micelle, the blue tail represents an alkyl chain of length  $m$ , while the orange tail represents an alkyl chain of length  $n$ .*

Equation 2-2 indicates that if the mixing of surfactants is ideal, the  $CMC_{mix}$  will be equal to the sum of the mole fraction of its constituent amphiphiles and their respective CMC values over the entire composition range. Therefore, the mixing of a binary system can be modelled by equation [2-3]. *Figure 2-5* shows a cross section of a binary mixed micelle consisting of monomeric surfactants with the only differentiating factor being the length of the alkyl chain. These binary systems of surfactants are all that will be assessed in this study.

#### **2.4. The Mixed Micelle and Gemini Surfactant Problem**

Even with the push for research on mixed systems due to their unique properties, there are many aspects that still need clarification. For example, the mechanism of mixed micelle formation is a debated topic, the schematic of possible mechanisms is presented in *Figure 2-6*. Scheme 2 is

the method proposed by Cui and colleagues in their research, as their NMR data suggested that there is a stepwise formation process where all of surfactant a and b will aggregate separately and collide to give the traditional mixed micelle, while the concerted one step formation has been the traditionally accepted mechanism.<sup>1</sup> This illustrates a gap in our knowledge of surfactant chemistry describing a phenomenon that has wide applicability in both the pharmaceutical and the consumer products field. Therefore, an in-depth understanding of the formation of mixed micelles and the phenomenon of solubilization are critical in these applications; this is an area where computational chemistry might shed some light as to the validity of the currently accepted mechanism versus the one recently advanced by Cui et al.<sup>1</sup> As well, in our case, understanding the behaviour of mixed systems of gemini surfactants may provide novel insights into their formation processes and in the mechanism of mixed micelle formation in general.

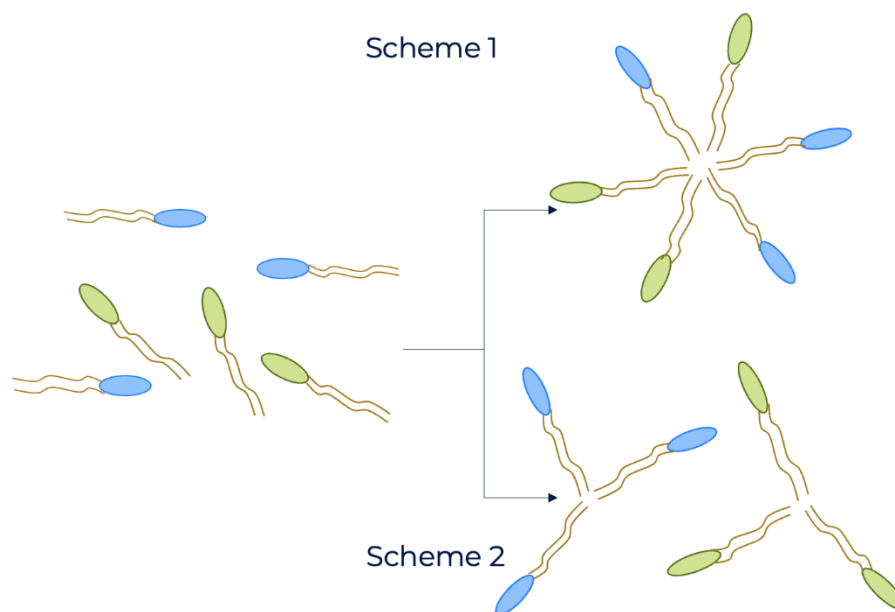


*Figure 2-6 - Proposed mechanisms of mixed micelle formations, the orange tail denotes an alkyl chain of length  $m$ , the blue head represents the two nitrogen heads connected by a spacer length  $s$ , and the green head represents the two nitrogen heads connected by a spacer length  $z$ .*

## 3. Computational Theory

### 3.1. Computational Chemistry

The foundation of theoretical chemistry lies in describing a system, for example, important questions such as; what are the particles? How many of each particle type do you have? What are the starting conditions (temperature, pressure, velocities, positions)? How do the particles interact? Finally, how does the system change over time i.e., what equations govern the dynamics all need to be addressed. When considering systems consisting of hundreds to millions of atoms, classical physics simulations such as molecular dynamics is often considered the method of choice. The classical method is the method of choice here, as quantum simulations would be too computationally expensive.

The study of n-body problems has been achieved through the use of Molecular Dynamics<sup>24</sup> using the GROMACS<sup>25</sup> package to handle such large molecular systems. Groningen Machine for Chemical Simulations (GROMACS) is a package used to run simulations of molecular systems using Newton's equations of motions solved numerically.<sup>25-27</sup> GROMACS was developed to investigate macromolecules in solution. In contrast to the Monte Carlo (MC) lattice method, it is seen as a more natural evolution of the system using parameters that will allow the components to move in a manner that reproduces translational motion rather than movements that must be coded into MC cycles that does not include dynamical information.

One of the big issues present in attempting to simulate an “infinite” system is the fact that systems are not infinite. A major point of contention in theoretical chemistry is that the computational approach can be heavily dependent on the methodology, such as the forcefields, and boundary conditions.<sup>28</sup> The choice of boundary conditions will give rise to artifacts depending

on the system studied. GROMACS in our study will employ the use of periodic boundary conditions. *Figure 3-1* is a top-down view along the z axis of a simple system consisting of a single micelle in water moving across the x axis, the center box is the one that has been built, the reflections alleviate the effects of hard boundaries simulating a pseudo bulk solution.

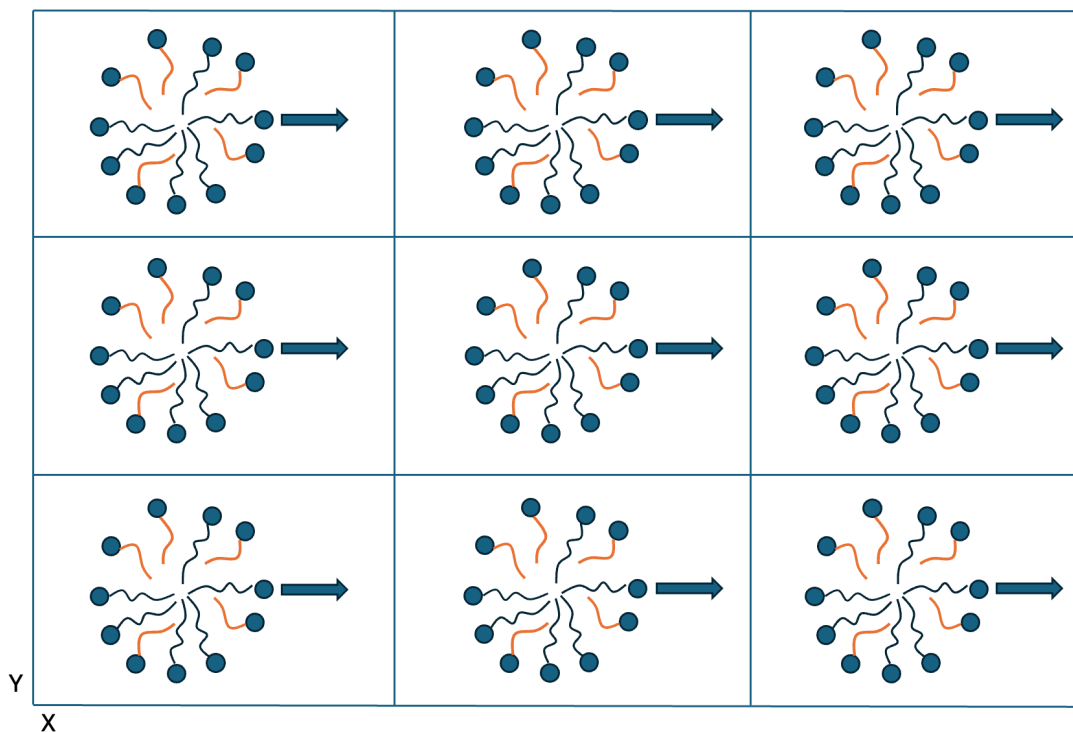


*Figure 3-1 - A simple system depicting periodic boundary conditions, the object in the center box as well as its motion is reflected periodically outwards in all directions to alleviate the effects of a hard boundary.*

The interactions (short/long ranged and inter/intramolecular) used in molecular dynamics is described as a forcefield. Each molecule is given its own force field parameterization that determines how the molecule will interact in the simulation space. A typical force field is the potential energy of the molecule  $U(\vec{r})$  as a function of the position ( $\vec{r}$ ) of  $N$  atoms. Equation 3-1 can be described by bonded interaction (bond length, torsions of bonds, and bond angles) and non-bonded interactions (Lennard-Jones interactions and a coulombic term).<sup>29</sup> Bonds and angles are described by a summation of harmonic potentials where its difference from a reference value i.e.

$b_o$ ,  $\theta_o$  is taken and multiplied by a spring constant. The torsional term includes improper dihedrals to ensure planarity of  $sp^2$  atoms. Lennard-Jones interactions are used to describe van der Waals interaction; and the coulombic term simply follows coulombs law. This simplified description of the system is known as a class 1 force field.<sup>29</sup> Equation 3-1 when translated to the molecule itself is shown in Figure 3-2.

$$U(\vec{r}) = (\sum_{Bonds} k_b (b - b_0)^2 + \sum_{Angles} k_\theta (\theta - \theta_0)^2 + \sum_{Torsions} k_\phi [\cos((n\phi + \delta) + 1)]^2)_{bonded\ interactions} + (\sum_{Non-bonded\ pairs} \left\{ \frac{A_{ij}}{r_{ij}^{12}} - \frac{C_{ij}}{r_{ij}^6} \right\}_{LJ} + \left\{ \frac{q_i q_j}{r_{ij}} \right\}_{Coulomb})_{non-bonded} \quad [3-1]$$

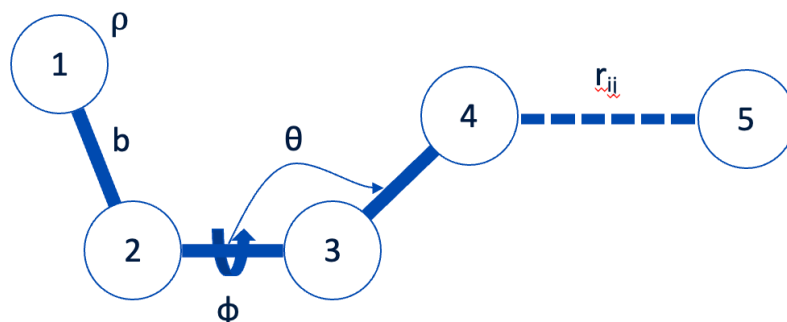


Figure 3-2 - Depiction of forcefield parameters considered in molecular dynamics (Pink et al.)

29

### 3.2. Computational Studies of Micellar Structures

Monte Carlo<sup>50</sup> and molecular dynamics have been used to successfully model surfactant systems. Burrows and his colleagues saw success measuring the electrostatics of a system of symmetric cationic gemini surfactants  $m=12$ .<sup>30</sup> The effect on the electrostatics and hydrophobic effects were monitored as a function of spacer length  $s=2,3,5,6,10$ , or 12. The aggregates of a conjugated polyanion was broken up upon the addition of the gemini surfactants which occurred as a result of interactions between the polyanion and the surfactant. Molecular dynamics suggest a good balance exists between the hydrophobic and coulombic effects as the spacer length is

increased past  $s=5$  which is responsible for the disruption of the polymer aggregates and the subsequent formation of the polymer/surfactant aggregates.

The development of a new united atom forcefield was used to study systems consisting of cetylpyridium bromide (CPB), investigated by Verma, adopted the GROMOS9654a7 forcefield and tailored it by comparing to experimental data.<sup>31</sup> The study aimed at producing data in good agreement with experimental and theoretical values, of water, 1-octanol, and the micelle. They observed a planar pyridinium ring for the CPB, as well, vibrational modes that were consistent with experimental data was observed. The molecular dynamics simulations showed a good stability of the micelle over a 100 ns simulation.

### 3.3. Radial Distribution Functions

Radial distribution functions will prove to be the key means of assessing the model. A radial distribution function or RDF describes how the density of a particle varies with respect to the distance  $r$  from a reference point in a system. This means normalizing the number of particles found in a sphere with radius  $r$  and a thickness of  $dr$ .<sup>32</sup> *Figure 3-3* represents a model for what a typical RDF looks like for a particle distribution of particles  $B$  at distances  $r_1$ ,  $r_2$ ,  $r_3$ , and  $r_4$  from a reference point (particle  $A$  in this case). From this model distribution the most dominant distribution is  $r_2$ , as the majority of particle  $B$  fall within this sphere.

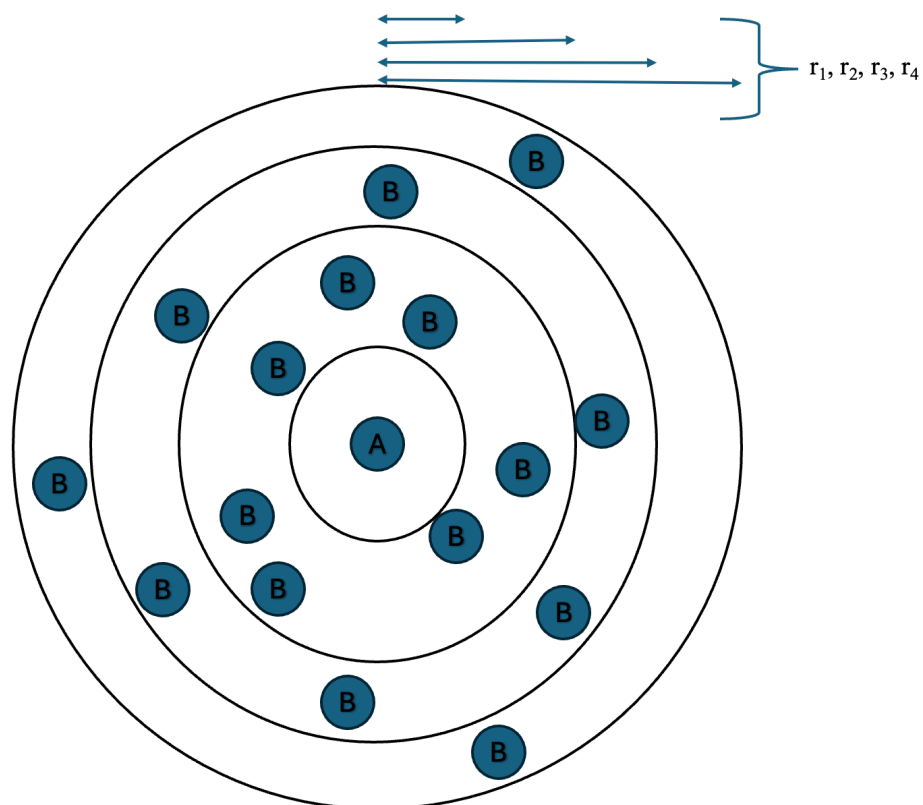


Figure 3-3 - Schematic showcasing the theory behind Radial Distribution Functions.

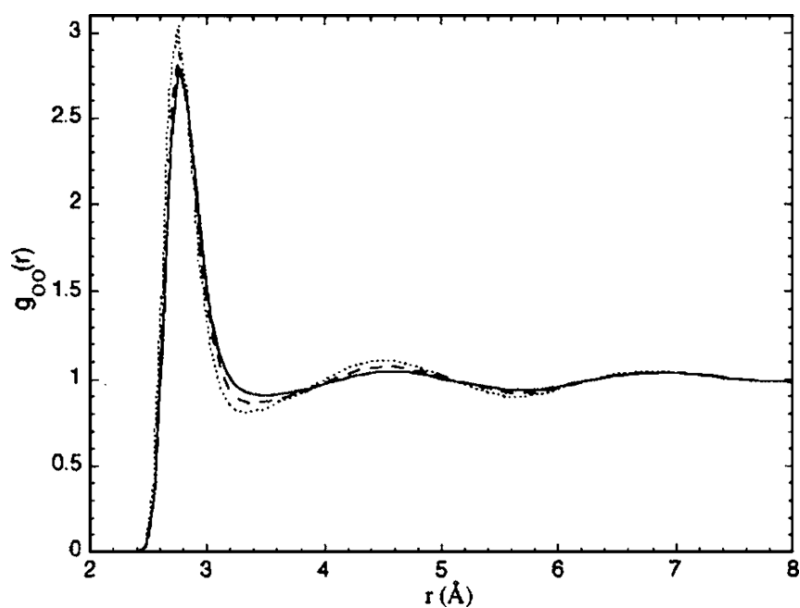


Figure 3-4 - oxygen-oxygen radial distribution function of SPCE water at 298K. The dotted, solid, and dashed lines correspond to the classical, quantum  $\text{H}_2\text{O}$ , and quantum  $\text{D}_2\text{O}$  results. (Hernández et al.)<sup>33</sup>

Contrasting this with an oxygen-oxygen RDF of water (*Figure 3-4*) the most dominant distribution occurs around 2.8 angstroms analogous to the max distribution shown in *Figure 3-3* ( $r_2$ ). There is no probability of finding another oxygen within 2.5 angstroms which corresponds to  $r_1$  in *Figure 3-3*. Finally, as the radius increases there are relative maxima and minima, a relative maximum of probability might be considered  $r_3$  in this case and a minimum would be  $r_4$ . This is the premise behind all structural analysis performed on the simulations.

## 4. Materials and Methods

### 4.1. Computational

#### 4.1.1. The Model

The simulations were performed on a Linux window (Terminal) using an Apple MacBook Air Laptop. The Terminal was used to access the Molecular Dynamics GROMACS package, which was hosted on the Digital Research Alliance of Canada system, *Narval*. The 3D structures of the surfactants and the associated *.mol* files required for computation were generated using Advanced Chemistry Development's ChemsSketch™ Software (version 2024.2.1).<sup>47</sup> The structures were uploaded to an online server called ATB<sup>34</sup>, that generated the molecular descriptions of the surfactants in a manner appropriate for GROMACS. The system files from ATB were further processed using Packmol<sup>35</sup> to generate the full molecular parameters for use with GROMACS. The study examined systems of symmetric 10 series surfactants with spacer lengths  $s = 2, 4, 6, 10$  (Table 1). Simulations have been performed with the united atom GROMOS54a7 forcefield, as the GROMOS forcefields have shown to have good agreement with molecular modelling of micelles.<sup>36</sup> The solvent for the model was a common water model, SPC/E. This water model is an appropriate model for the GROMOS54a7 forcefield..<sup>31,32,35–38</sup>

*Table 1 – Surfactant systems investigated in the present thesis with the number of water molecules used in the simulations.*

<b>Unmixed Systems at 298K</b>	<b>Mixed Systems at 298K</b>	<b>Large Mixed Systems at 298K</b>
<i>10 10-2-10 + 500 water molecules</i>	<i>5 10-2-10 + 5 10-6-10 + 500 water molecules</i>	<i>5 10-4-10 + 5 10-6-10 + 8000 water molecules</i>
<i>10 10-6-10 + 500 water molecules</i>	<i>5 10-2-10 + 5 10-10-10 + 500 water molecules</i>	<i>10 10-4-10 + 10 10-6-10 + 8000 water molecules</i>
<i>10 10-10-10 + 500 water molecules</i>	<i>5 10-4-10 + 5 10-6-10 + 500 water molecules</i>	<i>20 10-4-10 + 20 10-6-10 + 8000 water molecules</i>
	<i>5 10-6-10 + 5 10-10-10 + 500 water molecules</i>	<i>40 10-4-10 + 40 10-6-10 + 8000 water molecules</i>

Thus, the GROMOS54a7 forcefield was chosen, and the simulation box was defined and solvated. Unphysical forces were removed during energy minimization, and physical parameters such as the density, temperature, and pressure were equilibrated with respect to the canonical, and isothermal/isobaric ensembles (NVT, NPT).<sup>39</sup> The stability of the system was assessed via a plot of the potential energy against time, where a plateau represented a stable equilibration. The timestep was 2 fs, in an isotropic, cubic box with periodic boundary conditions equilibrated over 1 ns for the NVT and 1 ns for the NPT ensembles at 298 K, 1 g/cm<sup>3</sup>, and 1 atm. The equilibrated system was used as the starting point for the production runs over 10 ns. Interactions had a cutoff radius of 9 angstroms when treating nonbonding interactions, and the long range electrostatics were treated with the particle mesh Ewald method.<sup>40</sup> Depicted in *Figure 4-1* is the block diagram showing the full preparation and analysis of an MD run.

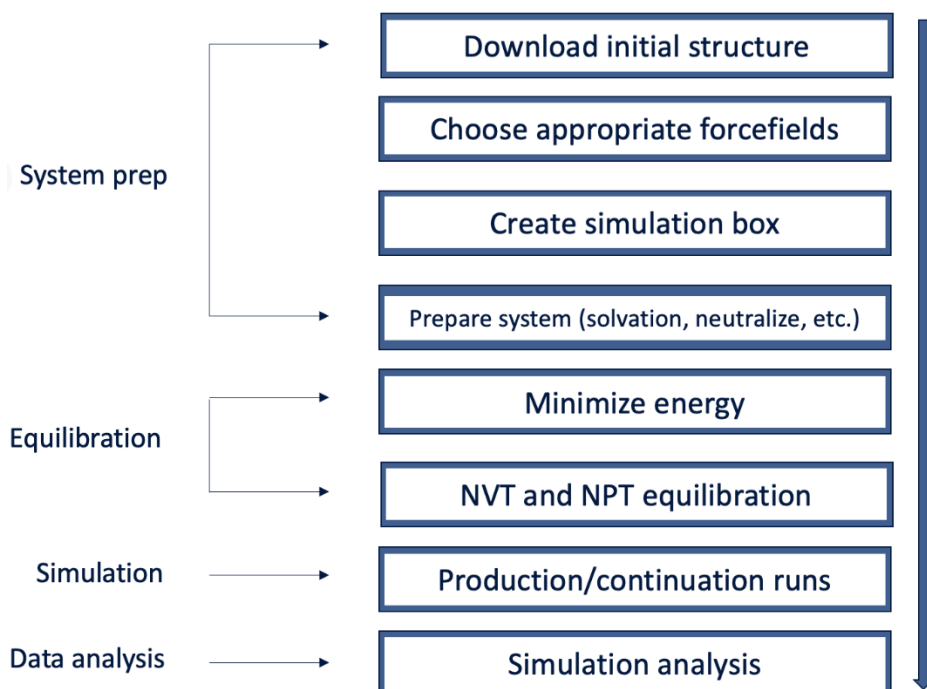


*Figure 4-1 - Block diagram of the preparation stages of the proposed model.*

#### 4.1.2. Simulation Radial Distribution Functions

Structural analysis was performed by RDFs using the GROMACS package. RDFs were used in assessing the effect that the length of the spacer chain has on the conformation of the chain. Potential changes to the conformation of the spacer chain were monitored by taking a point on the spacer chain as a reference point. Probability of distance were determined on  $m_1-s-m_2$  surfactants with the carbon in s compared to a carbon  $m_1$  in most cases.

The structural analysis of mixed systems was performed on a system of  $m-s_1-m$ ,  $m-s_2-m$ . A concentration of 20 mM calculated as shown in equation 4-1 and 4-2. Because systems in GROMACS don't operate near molar levels the calculation of concentration by converting the volume of water to number of water molecules meant that a concentration could be determined without accounting for the volume of the simulation box that is subject to change with GROMACS commands. The systems were initially simulated on a smaller scale and upscaled and compared to the smaller systems. This was undertaken at first, to save on computational power, reducing computer times, but also testing if there are any observable artifacts on a smaller system. The calculations are shown below:

$$\frac{0.02 \text{ mol } m-s-m}{1 \text{ L } H_2O} = 0.02M = \frac{0.02 \text{ mol } m-s-m}{1 \text{ L } H_2O} \cdot \frac{1 \text{ L } H_2O}{55.5 \text{ mol } H_2O} \cdot \frac{1 \text{ mol } H_2O}{N_A} \cdot \frac{N_A}{1 \text{ mol } m-s-m} = \frac{1.204 \cdot 10^{22} \text{ molecules } m-s-m}{3.34 \cdot 10^{25} \text{ molecules } H_2O} \quad [4-1]$$

$$\frac{x}{500 \text{ } H_2O \text{ molecules}} = 0.2M, x = 10 \text{ where } x = m-s_1-m + m-s_2-m \quad [4-2]$$

The RDFs performed were the same as that on a non-mixed system. *Figure 4-2* will serve as the reference for all RDFs performed. It is understood that all distribution functions consider

both inter and intramolecular distances, however, there are situations where the distribution function decouples the inter and intramolecular. For such circumstances closed square brackets will denote an RDF considering only intramolecular arrangements, while an open-ended bracket denotes a system that considers the reference atoms distribution concerning only intermolecular distances.

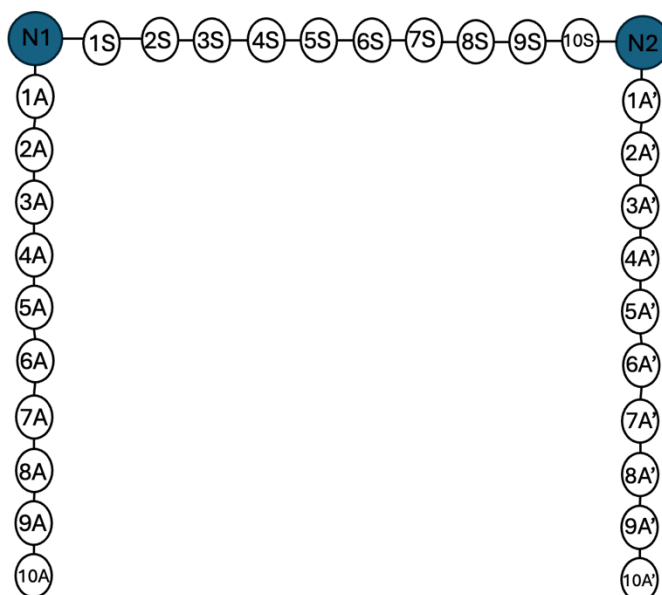


*Figure 4-2 - A numerical description of a 10-10-10 dimeric. Spacer chain carbons are counted from N1 and given the tag S, alkyl chain carbons are counted from their attached Nitrogen head and given the tag A for those attached to N1, and A' for those attached to N2.*

For example, a 1S-1A RDF concerns all 1A carbons with respect to 1S, while [1S-1A] is only the intramolecular distributions and [1S-1A) concerns 1S with all 1A save the one on its molecular framework.

### **4.1.3. Comparative Energetics Experiments**

Comparative energetics of the system was performed by assessing the potential energy of the system using the GROMACS package. The concentrations of a mixed system of 10-4-10 and 10-6-10 were increased in a set amount of water molecules. The water was held constant so that any changes to the potential energy can be attributed directly to the number of surfactants present. Finally the ratio of the surfactants was kept constantly at 1:1. This was done to observe potential deviations in linearity, if there is a change in the interactions of the system as a function of concentration a deviation should be apparent.

## 5. Results and Discussion

### 5.1. Non-Mixed Surfactant System to 2D <sup>1</sup>H NMR Experiments

This thesis first tests the model's accuracy by comparing to experimental 2D-<sup>1</sup>H NMR data. NMR experiments are done by immersing the molecule of interest in a strong magnetic field inducing the nuclei of the molecule to align with the magnetic field. These nuclei are then excited to a higher energy state and the relaxation of these nuclei are then measured to reveal the chemical environment of those nuclei. The two-dimensional NMR experiment will correlate two nuclei in a system based on through-space or through-bond interactions. Nuclear Overhauser Effect Spectroscopy or NOESY show correlation signals caused by dipolar cross-relaxation of protons. This relaxation signal is typically observed when the two nuclei are in proximity of each other within 0.5 nm or less. The strength of these peaks is inversely proportional to  $r^6$  where  $r$  is the distance between the nuclei. This has been used in the study of biomolecules simply due to the complexity of the structure.<sup>41-43</sup> The rotation frame analog of the NOESY is known as the ROESY experiment. While the experiments differ slightly in the pulse sequences used, the interpretation of the cross-speaks is the same – that is a through-space dipolar interaction between the protons where the protons are in a spatial proximity of 0.5 nm to one another.

The trials from MacNeil et al. reports a “bending back” of the spacer chain above  $s = 4$ . In their experiments, 20 mM concentrations of the symmetric 10 series dimers were used for the ROESY experiments.<sup>51</sup> The presence of ROESY cross peaks demonstrate H-H interactions within 5 angstroms or 0.5 nm, and the presence of these peaks were used qualitatively to interpret conformations of the aggregates. The paper reports a cross peak between the  $\beta$  of the spacer chain to the  $\gamma$  carbon of the alkyl chain is only observed with the 10-10-10 surfactant and this data can

be used to validate the correlations derived from the GROMACS simulations. As an example, *Figure 5-1* is an RDF of the  $\beta$  spacer to  $\gamma$  alkyl chain (2S-3A). In the figure it can be observed that only 10-10-10 has a probability peak within 0.5 nm.

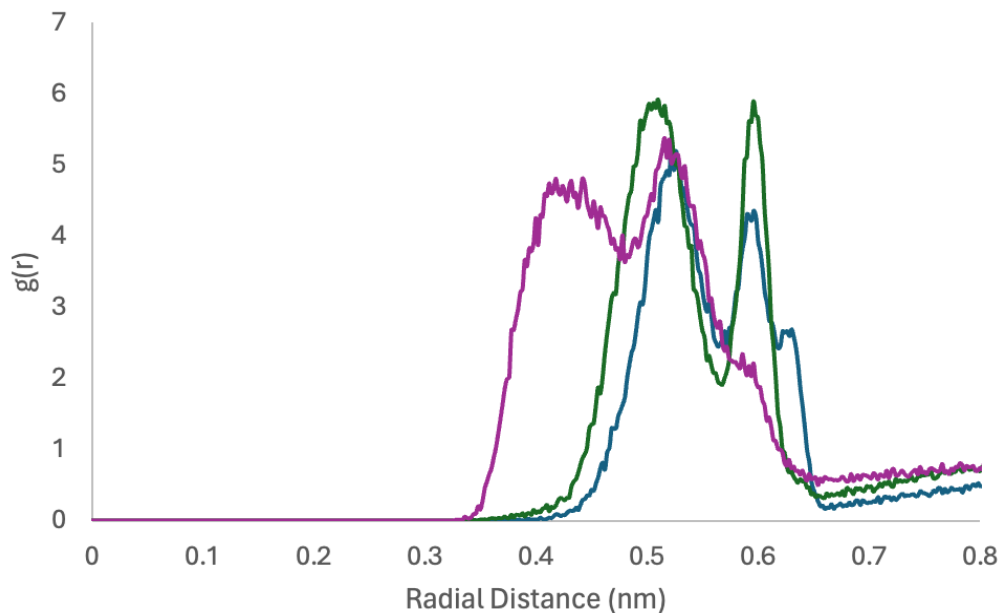


*Figure 5-1 - Radial distribution function of 2S-3A. The blue line represents the 2-length spacer chain, green represents  $s = 6$ , and purple represents  $s = 10$ .*

The ROESY data cannot indicate the exact distance, only if they are within 0.5 nm, since all alpha spacers to alpha chain show cross relaxation peaks it can be assumed they are within 0.5 nm. *Figure 5-2* predicts distances under 0.5 nm for all alpha spacer to alpha chain carbons. The RDF of all trials are within the 5-angstrom limit, with peaks at around 0.25 nm. The 0.25 nm distance was tested with an optimized structure of 10-6-10 in Gaussian 09<sup>44</sup> using the hybrid DFT method b3lyp<sup>45</sup> with the 6-31+G(d) basis set.<sup>48</sup> Despite being a gas phase optimization with chlorine anions left out to save on computational load, the distance was still in good agreement (0.249 nm). It can be observed that there is not a spectrum of probability, only a single sharp peak suggesting little room for flexion in either the alpha carbon of the spacer chain or the alpha of the chain. Although swamped by the extreme region of probability, the intermolecular distance can be

observed clearly from the distributions. It does seem to show that the next nearest alpha chain carbon can exist in a closer conformation suggesting tighter packing proportional to the spacer chain length. This is also shown in **Section 5.3** to minimize the chance that this is an artifact of a smaller system size.

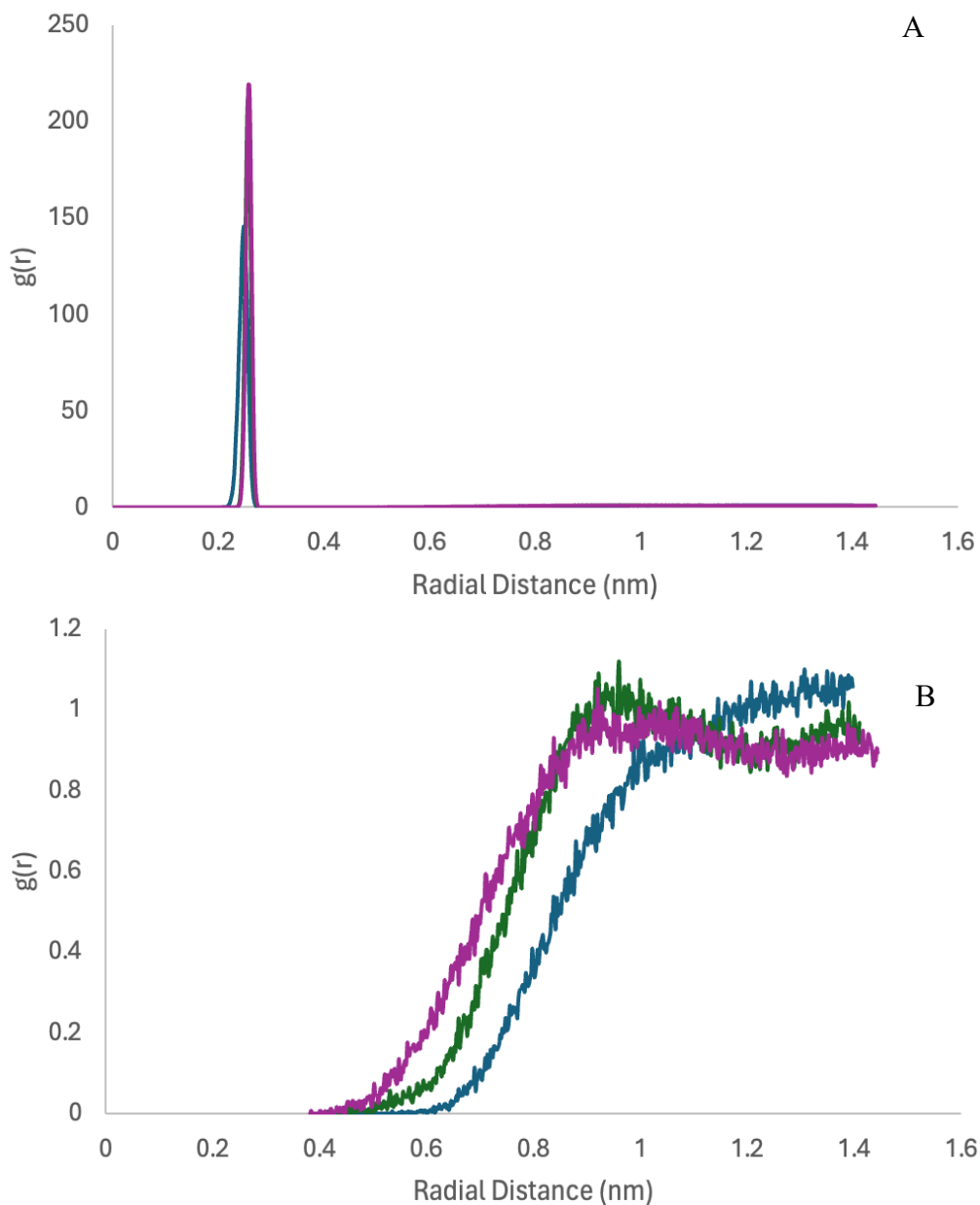
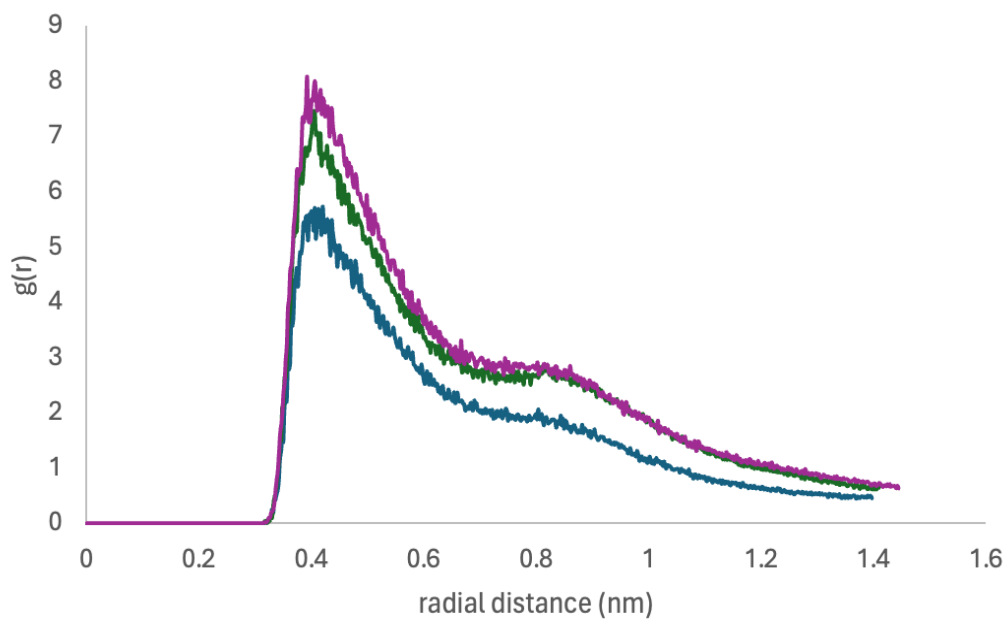


Figure 5-2 - An RDF of 1S-1A and (B) the RDF for [1S-1A]. The blue line represents  $s = 2$ , green represents  $s = 6$ , and purple represents  $s = 10$ .

The radius needed to find an intermolecular alpha chain carbon is consistently smaller as a result of the spacer chain. Along with this, a RDF of the terminal carbon (10A) to terminal carbon (10A') seems to indicate this as well. With increasing spacer chain length, the distribution function shows a greater distribution of terminal carbon to terminal carbon, though the shape of the graph remains the same (*Figure 5-3*), suggesting the aggregation becomes tighter with increasing spacer chain. The graph also suggests a broad degree of rotational freedom considering there is no clear separation between the inter-intramolecular distribution. The rotational freedom is only strengthened by *Figure 5-5 (B)*.



*Figure 5-3 - Radial distribution function of 10A-10A'. The blue line represents the 2-length spacer chain, green represents  $s = 6$ , and purple represents  $s = 10$ .*

As well, the beta spacer chain seems to be in good alignment with the delta spacer chain experimental distances. *Figure 5-4* shows that only for  $s = 10$ , would a ROESY show up in a spectrum. Interestingly, the model presented from RDFs on a system size this large indicates that the spacer chain hasn't back bent, at least to the degree of the 10 spacer. This may of course be a flaw

of the model, although it may be possible that the bending of the model is not occurring in a way that has been traditionally described. Typical to dimerics, aspects about them remain unresolved, and the RDFs bring us no closure on the matter of their formation, though they do pose a question of how they aggregate. This question is only exacerbated by *Figure 5-5* which is an RDF of the alpha spacer and the omega chain carbon.

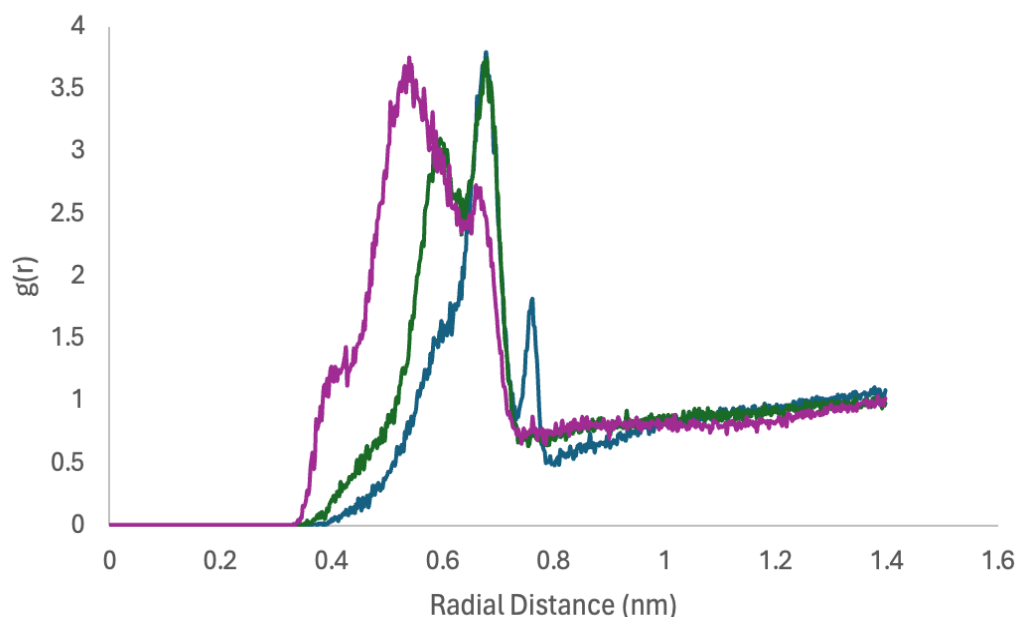
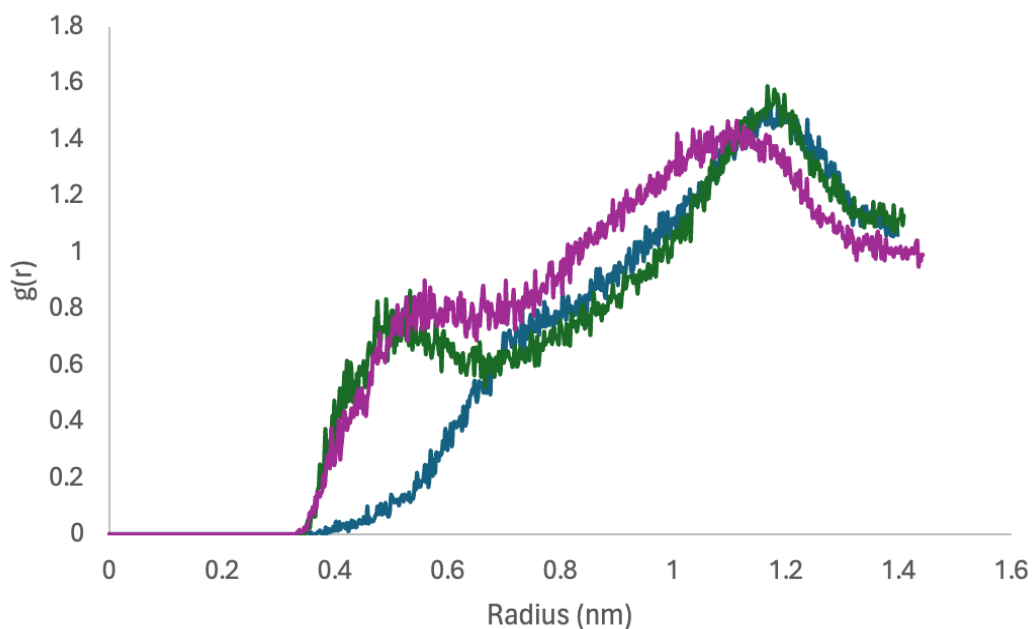


*Figure 5-4 - Radial distribution function of 2S-4A. The blue line represents the 2-length spacer chain, green represents  $s = 6$ , and purple represents  $s = 10$ .*

*Figure 5-5 (B)* suggests there may be artifacts when assessing the terminal chain carbons. *Figure 5-5 (A)* is an RDF of the alpha spacer to omega chain carbon. It can be seen that as  $S$  increases the aggregation changes when  $s$  is greater than 4. This is in line with experimental data, where the data shows a conformational change above  $s = 4$ , until the intra and intermolecular interactions are decoupled and taken as separate RDFs (*B*). Upon decoupling the interactions of 10-6-10 it is observed that intermolecular distributions appear before intramolecular. This is puzzling when one expects a well-defined micelle to have the chains oriented towards the center.

The steric hinderance should allow no chance of an orientation where the terminal carbon intermolecularly adopts a conformation in closer proximity to the alpha spacer than its own omega carbon. The probability peak in *Figure 5-5 (A)* at 0.125 nm is in agreement with the optimized structure of 10-6-10 (0.127 nm for 10-6-10 optimized with b3lyp 6-31+g(d)) further supporting the validity of the model with the exception of the intermolecular proximity. What the decoupled alpha-TC RDF does showcase (*Figure 5-5(B)*), is the fluidity or rotational freedom of the alkyl chain which was hinted at in *Figure 5-3*. The broadness of *Figure 5-5(B)* can be attributed to the omega carbon of the alkyl chain (10A) while the alpha spacer is inferred to be rigid considering *Figure 5-2(A)*. *Figure 5-6* provides a proposed aggregation scheme that may account for this anomaly, since these aggregates are not well-defined micelles aggregate conformations where the chain of a surfactant may face toward the spacer of another surfactant. This conformation is not dominant of course, and the trend of the distribution function in *Figure 5-5(B)* supports that as you go further out radially it becomes increasingly likely that an intermolecular terminal carbon exists.



A

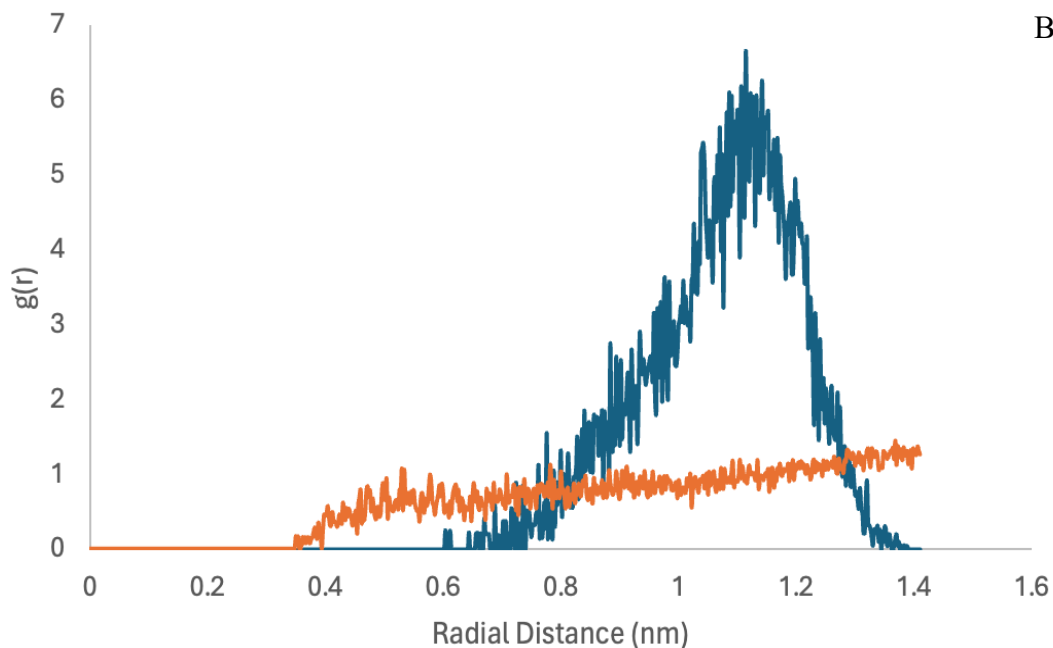


Figure 5-5 - (A) RDF corresponding to 1S-10A. The blue line represents the 2-length spacer chain, green represents  $s = 6$ , and purple represents  $s = 10$ . (B) 1S-1A RDF of 10-6-10 that has had its inter and intramolecular interactions decoupled. The blue line represents  $[1S-10A]$ , while the orange line represents  $[1S-10A]$ .

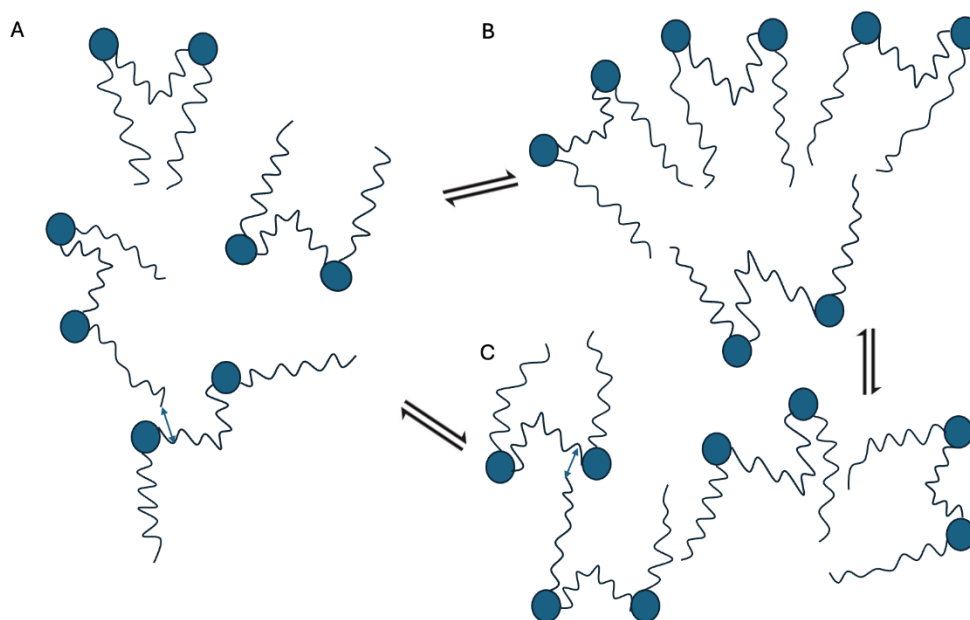
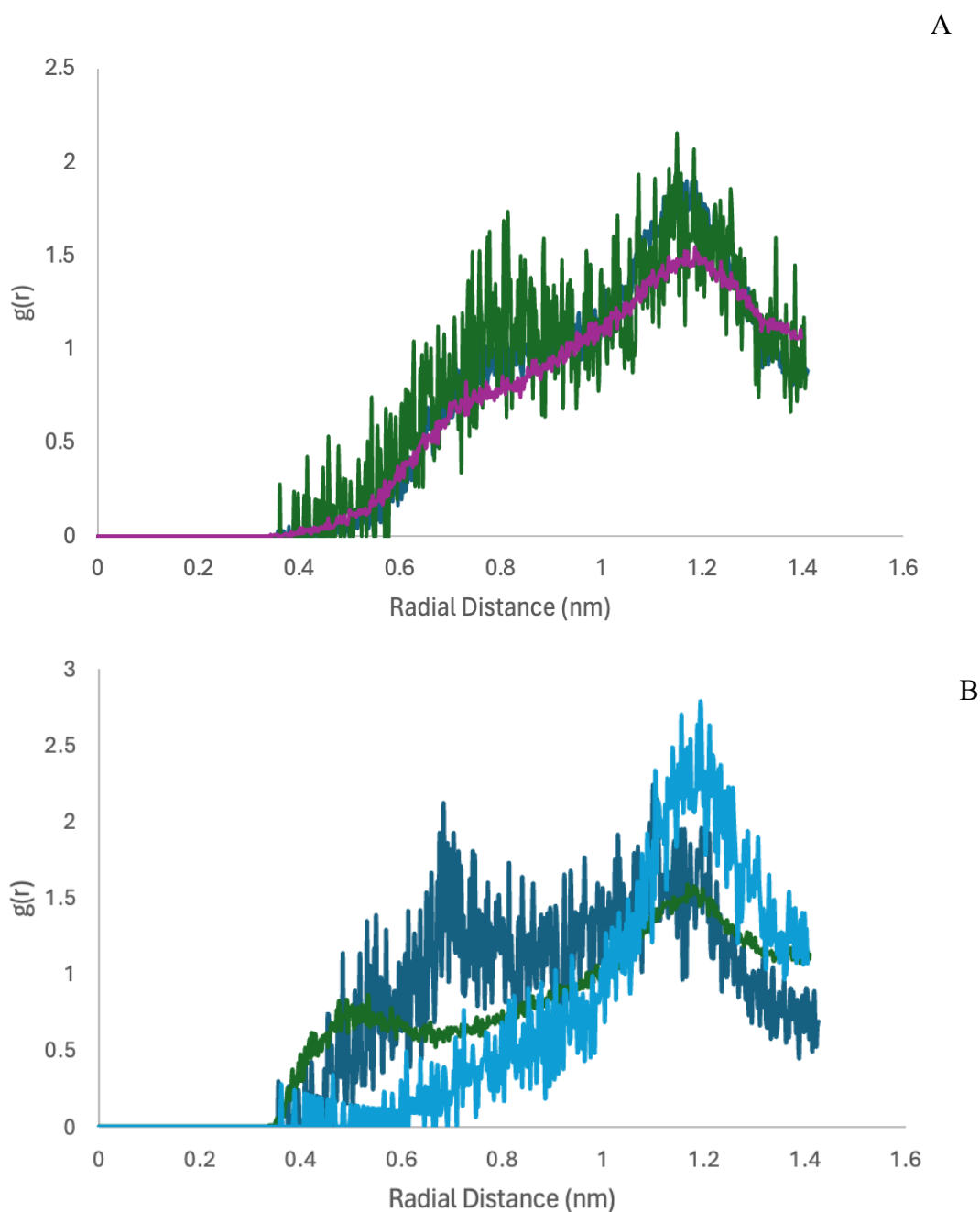


Figure 5-6 - Proposed aggregation scheme of a random dispersion of 10-10-10 (A) into a typical aggregation (B) and a semi aggregate (C). The model serves to provide a reasoning for the appearance of terminal carbons within a shorter distance than the intramolecular distance denoted by the arrows.

Although, the intermolecular RDF trend itself does align with what would be expected experimentally, the anomaly of the intermolecular proximity may merit a closer investigation.

## 5.2. Mixed Surfactant System to a Non-mixed System

Once the accuracy of the model to predict conformational trends from experimental data was determined, the system was modified to a C(5, 2), mixed system surfactants. The same RDFs were taken as its unmixed counterpart and the RDFs were observed to determine if the introduction of a new dimeric affected the conformation. The distribution functions become much noisier with the addition of the second surfactant to the system, this of course may be due to the aggregate structures “disruption” as the aggregate is no longer composed of only the surfactant of interest. This may be a factor but more likely, is the fact that there are 5 surfactants in solution. In **Section 5.3**, when the system is increased to 80 surfactants (40 of each), the distribution clears up. This may indicate that for smaller systems, longer run times may be required for the equilibration to reach a smoother profile of the RDFs. The trends experienced in the mixed system remain largely the same as can be seen in *Figure 5-7 (A)* where a 10-2-10 terminal carbon to alpha spacer RDF have the same shape, there are outliers that might be rectified in a larger system. One such outlier is seen in *Figure 5-7 (B)* which shows that the same RDF for a 10-6-10 does change with the addition of a 10-10-10 surfactant. A region from 0.600 nm to 0.630 nm becomes nearly as dominant a configuration as the intramolecular distances. Of course, considering *Figure 5-3* which suggests a tighter aggregation proportional to  $s$ , it is possible that 10-6-10 is forced into a semi binding aggregate while the 10-10-10 lies in the traditional aggregate.



*Figure 5-7 - Figure 5-7: (A) 1S-10A RDF of 10-2-10 in solution with a secondary surfactant. The blue line represents a 10-2-10 in solution with 10-10-10, green represents a mix with 10-6-10, and purple represents the unmixed 10-2-10. (B) 1S-10A RDF of 10-6-10 in solution with a secondary surfactant. Dark blue represents a mix with 10-10-10, the turquoise represents a mix with 10-2-10, and the green represents the unmixed 10-6-10.*

The model, when considering how the beta spacer carbon spatially exists relative to other carbons, remains valid. *Figure 5-9* remains consistent for the unmixed solution suggesting the model remains useful in providing information about the  $\beta$  carbon to the  $\gamma$  and  $\delta$  chain carbon (2S-2A and 2S-4A). *Figure 5-9 (B and C)* also remain consistent with the trends of their unmixed counterparts in reference to the relative position and number of peaks.

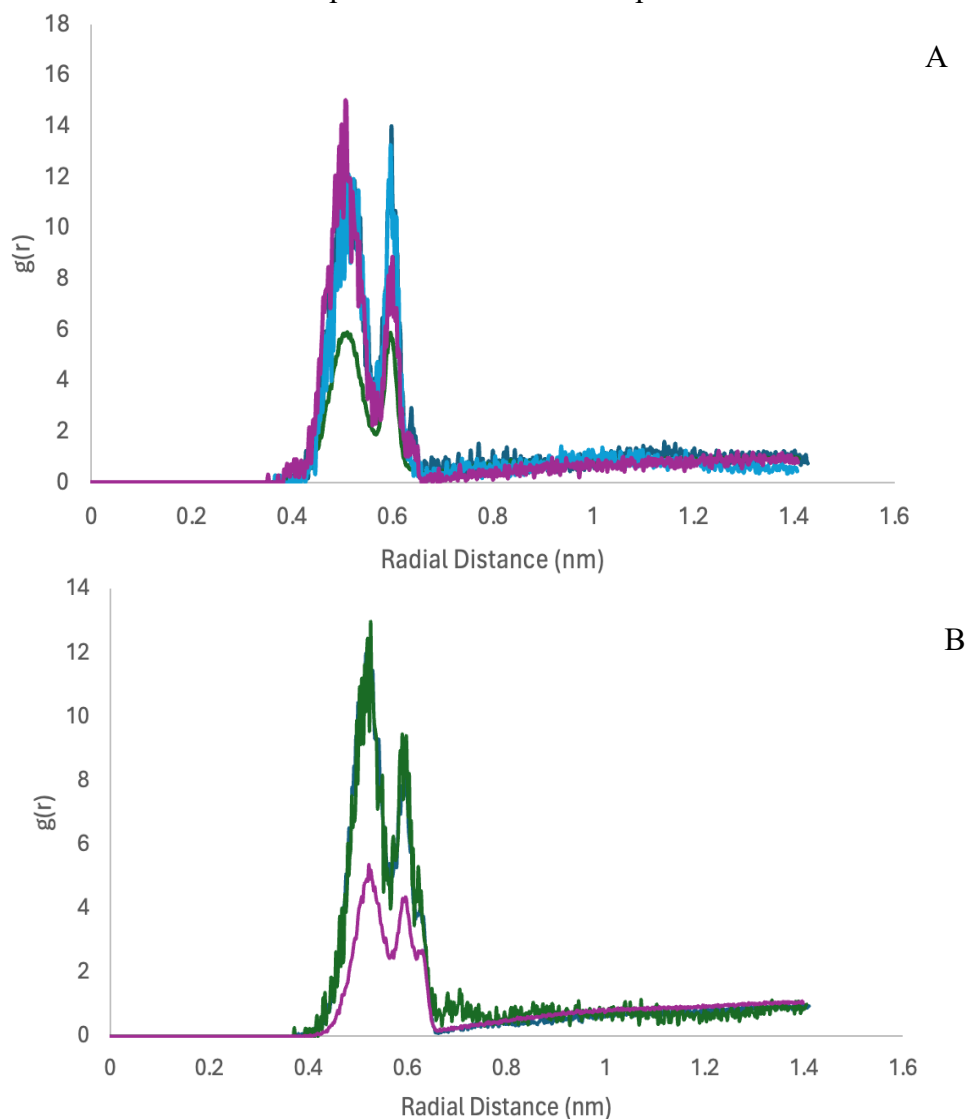


*Figure 5-9 - (A) 2S-3A RDF of 10-6-10. The green line represents the unmixed 10-6-10, while dark blue, turquoise and purple are mixed systems with 10-10-10, 10-2-10 and 10-4-10, and (C) 2S-3A RDF of 10-2-10. The purple line represents the unmixed 10-2-10, while the blue and green line represent a mixed system with 10-10-10 and 10-6-10.*

### 5.3. System Size Effects on a Mixed System of 10-4-10:10-6-10

In this section, the impact of the size of the system upscaled on the distribution functions is presented and discussed. For this comparison only one system size was chosen due to the time constraints of the project. 10-4-10:10-6-10 was chosen simply because there were no unforeseen interactions when the systems were mixed, as they behaved as they did in the unmixed simulations, meaning any differences observed, ideally would be due to increasing the system size and no other interactions. RDFs were calculated on a system containing 40 10-4-10 and 40 10-6-10 and compared to the systems containing 5:5 to expand upon data that may have been incomplete. *Figure 5-10 (A)* is one such example of that. The maximum distribution of the 10-4-10 alpha spacer to alpha chain in both systems remain at 0.244 nm, but the peak broadens from a range of 0.232-0.254 nm to 0.230-0.258 nm. The same can be said for *Figure 5-10(B)*; the maximum peak of 10-6-10 alpha spacer to alpha chain is 0.256 nm, yet the range of the distribution upon increasing the system size is increased from 0.234-0.276 nm to 0.224-0.278 nm. For both the 10-4-10 and 10-6-10 the overall trend has remained the same, a peak early in the distribution, a region of no conformations due to the extreme steric hinderance that must be overcome to either bring an intermolecular alpha carbon within proximity, or the extreme strain that would be needed to stretch an intramolecular [1S-1A] interaction, and of lower probability of denoting the distance of an alpha spacer to an intermolecular alpha chain. Still the graph in *Figure 5-10* does suggest what has been seen experimentally on a microscopic scale, that is, more flexibility in the alpha spacer chain with increasing spacer length.

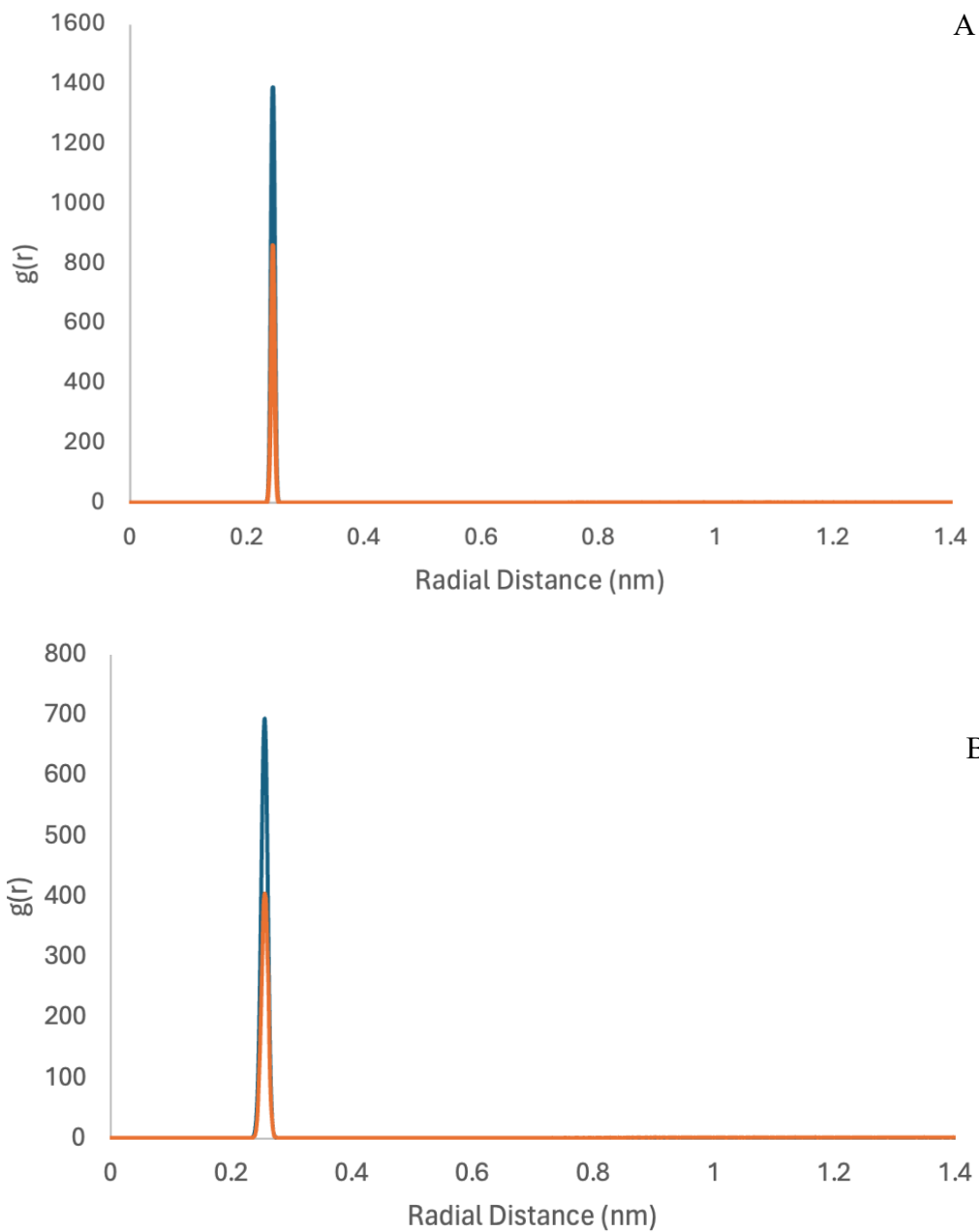
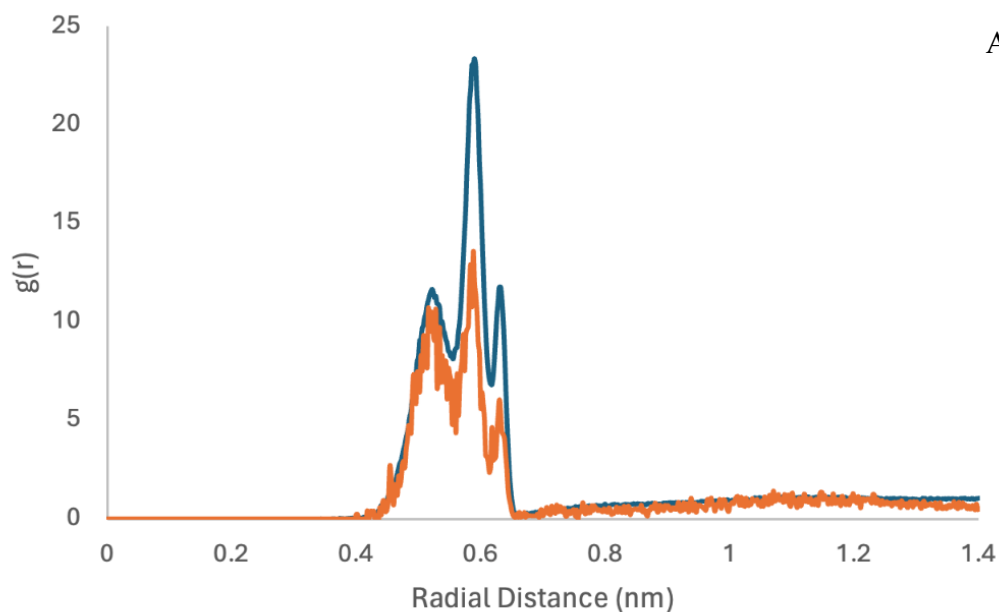


Figure 5-10 - (A) 1S-1A RDF of 10-4-10 in a mixed system with 10-6-10 (B) 1S-1A RDF of 10-6-10 in a mixed system with 10-4-10. The blue line is the 40:40 while the orange is the 5:5 system.

The model remains consistent in its predictive power of the  $\beta$  spacer conformation. *Figure 5-11* is the RDF of the  $\beta$  spacer to  $\gamma$  chain for both the 10-4-10 (*A*) and the 10-6-10 (*B*). It should be noted that according to the RDFs presented, both 10-4-10 and 10-6-10 have regions within 0.5 nm indicating they should be observable in the NMR. The peak of the RDF for both, however, do still lie outside of 0.5 nm, 0.522 nm for the 10-4-10 and 0.520 nm for the 10-6-10 respectively. This is unlike that of the 10-10-10 system that has a peak before 0.5 nm (*Figure 5-1*). There is a different structure reported for a 10-4-10 2S-3A than for all other 2S-3A, that being a 3-peak distribution as opposed to the 2-peak that has been observed for all 2S-3A thus far. What conformations might be adopted as shown by the distribution cannot be accurately commented on without further research although it does serve as a diagram for not only the richness of the system, but the unknown qualities of surfactant systems. For comparisons to experimental data, relative maximums may be the most important points of interest.



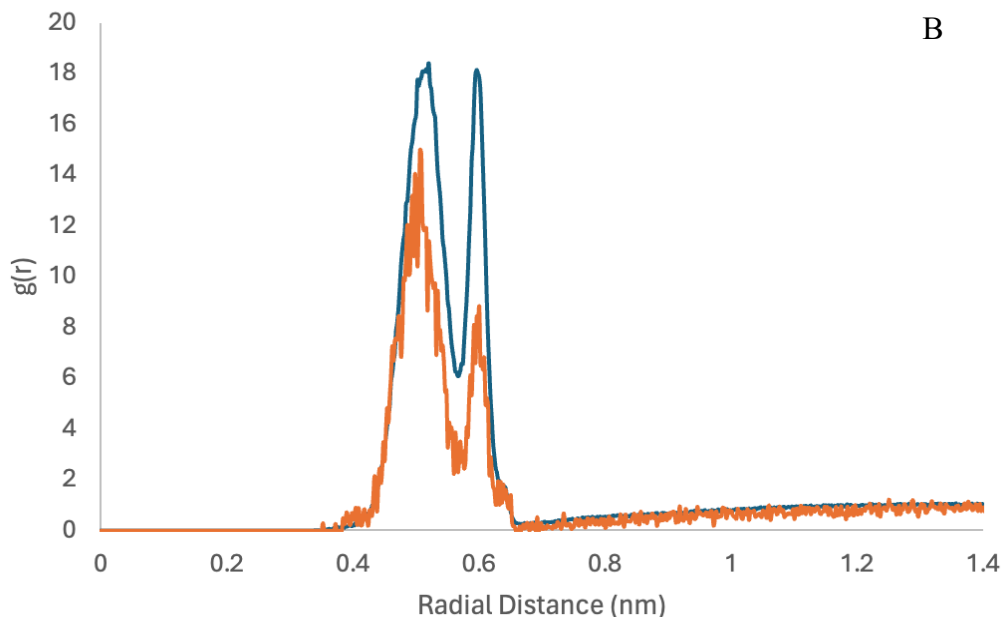


Figure 5-11 - 2S-3A of a 10-4-10 (A) and a 10-6-10 (B). The blue line represents a system size 40:40, and the orange line represents a system size 5:5.

Perhaps most indicative of the impact of system size is seen in *Figure 5-12*. The 10-6-10:10-4-10 1S-10A when considering the 10-6-10 in solution shows the typical bump in probability from 3.3-0.55 nm is not present in the 5:5 system, this shows a loss in intermolecular data. Troubling as this bump seems to be it puts on clear display the loss of intermolecular data with the loss of system size. Although, this bump is clearly present from a system size consisting of 10 of one type of surfactant, *Figure 5-5*, it would seem that the system size of 10 surfactants is suitable for interactions, though box size must also be considered, as can be seen in *Figure 5-12*. The 5:5 system cuts off abruptly, leaving the 2 nm of data showing how likely an intermolecular terminal carbon is to exist outside the intramolecular distance, which does agree with the typical aggregation proposed in *Figure 5-6(B)*.

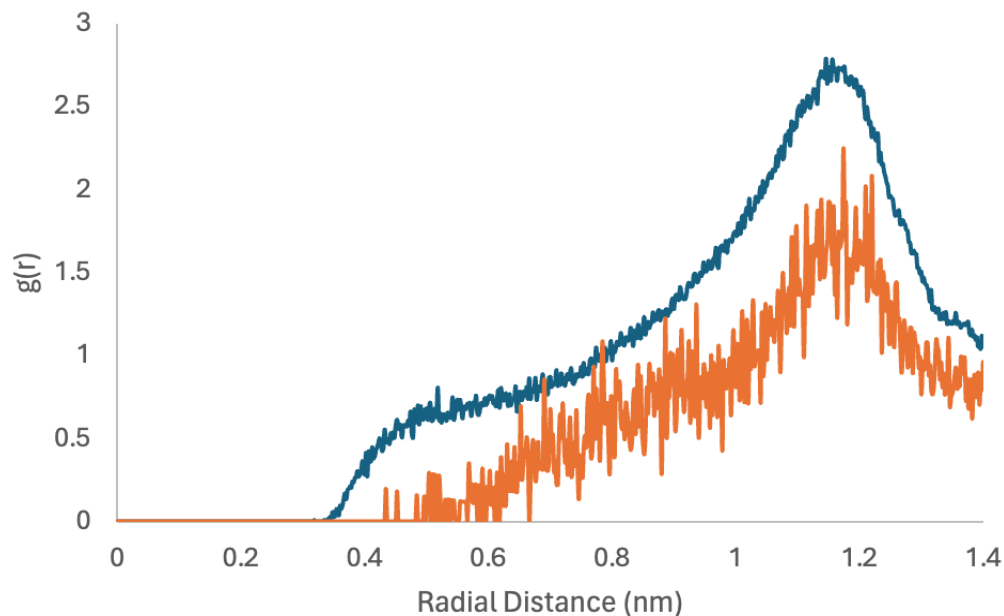
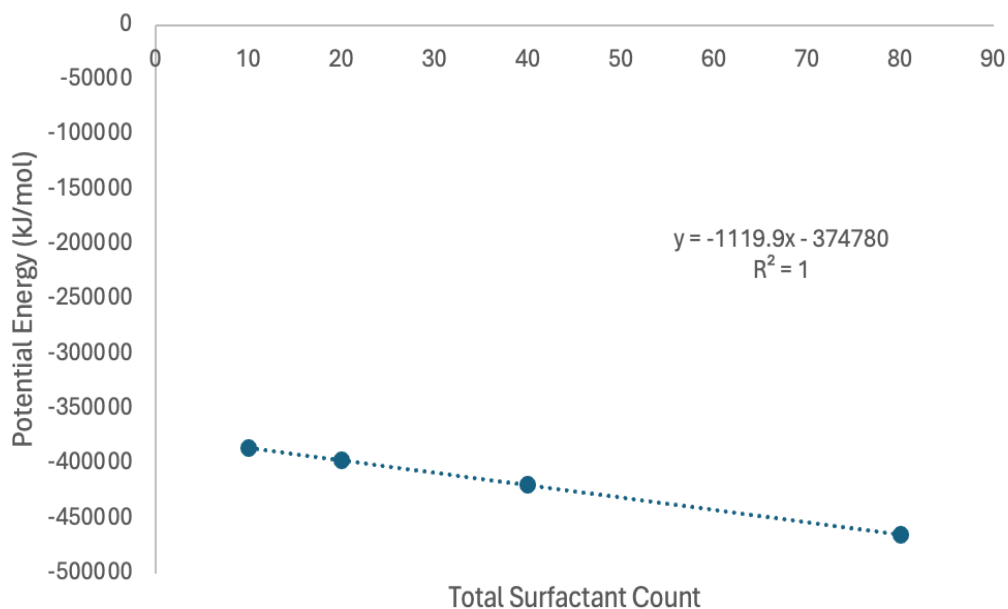


Figure 5-12 - A 10-6-10 RDF of 1S-10A in a mixed solution with 10-4-10. The blue line represents the 40:40, while the orange represents 5:5.

#### 5.4. Energetics Comparison of 10-4-10:10-6-10

Finally, the energetics of the system will be assessed. Though there were some potential artifacts such as those seen in *Figure 5-7* and *Figure 5-8* the consensus is that our model predicts a system that is mixing ideally, otherwise the distribution functions might have changed more drastically upon adding a secondary component. Though, preliminary ITC work suggests the system is not mixing ideally, but this test has not been repeated, and so further tests must be done to confidently assert the mixing as ideal or nonideal. To this end, systems of 5:5, 10:10, 20:20 and 40:40 were assessed in 8000 water molecules.

The average of the potential energies after a 10 ns mdrun was taken as the potential energy of the system. The error bars on the system are considered nonsignificant, as shown in *Figure 5-13* the bars aren't visible, this also shows that the system is at a well behaved equilibrium. *Figure 5-13* shows the trend as the number of surfactants increase. The trend is linear, showing no sign of deviation, suggesting there is no change in the energy with respect to the system size.



*Figure 5-13 - Potential energy of a 10-4-10:10-6-10 system as a function of surfactant count.*

## 6. Conclusions and Future Work

### 6.1. Conclusions

The model presented has been successful in modeling the conformation of the beta carbon to the delta carbon of the chain. RDFs of the 2S-3A and 2S-4A showing the peak probabilities in regions below 0.5 nm for  $s = 10$ . Intramolecular aspects aside from the bending of the interchange arm are consistent with what is expected of a quantum treatment of the molecule, i.e., the distance between the alpha spacer to alpha chain (1S-1A) having a distance of around 0.25 nm and the DFT geometry optimization of 0.249 nm. As well, rotational freedom moving further from the nitrogen head groups, in particular the 10A and 10A' carbons supporting the Gruen model.

The potential energy assessment in **section 5.4** suggests an unphysical result when considering the least concentrated simulation is 1.25 mM (below the CMC of the 10-4-10:10-6-10 system). Due to the random dispersion of the molecules in the simulation, the minimum conformation observed may in fact not be the global minima (micellization may not have occurred).

The model loses little in terms of the intramolecular interactions from the size of the system, although there is a loss of intermolecular interactions. The model can be used to decouple intramolecular interactions from intermolecular interactions, which may provide novel insight into the conformational analysis of molecules across multiple fields of chemistry. Therefore, this model may see use in ascertaining intramolecular interactions even at small system sizes with reasonable accuracy provided the concentration is above the CMC. In the case of providing intermolecular data the system size must be increased to minimize the chances at missed interactions.

Thus, the study presents a model that is consistent with experimental conformation data, but needs further study before commenting on the energetics of the system. The model is serviceable at small system sizes if assessing only the intramolecular framework, however, caution must be exercised when attempting to assess intermolecular data, as prominent interactions may be lost in cutting the system size down. Admittedly, resolution either the intermolecular, and intramolecular spectra can be improved by decoupling the spectra.

## 6.2. Future Work

This work details primarily, a computational review on the behaviour of mixed system aggregates consisting of a system of two gemini surfactants. The conformational behaviour and energetics will be compared with NMR and ITC measurements to assess the validity of computationally simulated systems of mixed gemini surfactants. Of course it is the importance of micelles across the different branches of chemistry that ensures we must continue to investigate mixed micellar systems. Once we determine the accuracy of computer simulated mixed gemini surfactants systems, the focus can shift towards applying the same model to asymmetric systems.

To further test the accuracy of the model, the  $\beta$  carbon must be tested against other members of the  $n\text{-CH}_2$  envelope. It needs to be determined how well RDFs of the  $\beta$  spacer predict the conformational behaviour or if the model begins to fail as we begin to test further distances. Preliminary ITC work suggests a nonideal mixing of N,N'-bis (dimethylalkyl)- $\alpha,\omega$ -alkanediammonium dibromides. This nonideal mixing begs the question of assessing the same RDFs performed in this study on families of dimers that known to not ideally mix. Indeed, contrasting the conformational behaviour observed in this study may provide a means for structure performance relationships that were previously impossible. Finally, testing for the probability

bump suggesting close proximity of the  $\alpha$  spacer (1S) to an intermolecular  $\omega$  carbon (10A) experimentally, can be performed and compared to future MD simulations. In short more RDFs must be performed not only on this family of surfactants, but new families must be included.

Energetics of the model, while not the focal point of the model suggests that increasing the concentration of the system, does not change the internal energy in a way besides scaling the energy. The lack of deviation from a linear curve of potential energy would suggest that there aren't more favourable conformations adopted with a more concentrated system. The CMC of the simulations is above that of the smaller system studied. The energetics of the system seem unphysical when considering this, and so more simulations must be run to determine if any of the results obtained are unphysical. As well, a surfactant/water ratio energetics calculation could be performed to determine the validity of the results presented in **section 5.4**.

Varying the ratio of the systems in this study may provide new insight into both the conformational behaviour, but more importantly potential energy of the system. In varying the ratio of the system, trends presented in the simulation may show correlation to the ITC, providing another means of linking the experimental and theoretical field of surfactants. Further ITC work must be done to establish a trend in the change of the CMC for a 10-4-10:10-6-10 system, as the ratio of the system is shifted from a ratio of 1:1. Further down the line, the potential energy of ideally mixed surfactant aggregates might be tested in the same manner as this system, monitoring the change in the potential energy curves between nonideal and ideally mixed systems.

## 7. REFERENCES

- (1) Cui, X.; Jiang, Y.; Yang, C.; Lu, X.; Chen, H.; Mao, S.; Liu, M.; Yuan, H.; Luo, P.; Du, Y. Mechanism of the Mixed Surfactant Micelle Formation. *J. Phys. Chem. B* **2010**, *114* (23), 7808–7816. <https://doi.org/10.1021/jp101032z>.
- (2) Kumar, N.; Tyagi, R. Industrial Applications of Dimeric Surfactants: A Review. *Journal of Dispersion Science and Technology* **2014**, *35* (2), 205–214. <https://doi.org/10.1080/01932691.2013.780243>.
- (3) Söderman, O.; Stilbs, P.; Price, W. S. NMR Studies of Surfactants. *Concepts Magnetic Resonance* **2004**, *23A* (2), 121–135. <https://doi.org/10.1002/cmra.20022>.
- (4) Israelachvili, J.; Ruths, M. Brief History of Intermolecular and Intersurface Forces in Complex Fluid Systems. *Langmuir* **2013**, *29* (31), 9605–9619. <https://doi.org/10.1021/la401002b>.
- (5) Kang, W.; Mushi, S. J.; Yang, H.; Wang, P.; Hou, X. Development of Smart Viscoelastic Surfactants and Its Applications in Fracturing Fluid: A Review. *Journal of Petroleum Science and Engineering* **2020**, *190*, 107107. <https://doi.org/10.1016/j.petrol.2020.107107>.
- (6) Raffa, P.; Broekhuis, A. A.; Picchioni, F. Polymeric Surfactants for Enhanced Oil Recovery: A Review. *Journal of Petroleum Science and Engineering* **2016**, *145*, 723–733. <https://doi.org/10.1016/j.petrol.2016.07.007>.
- (7) Menger, F. M.; Keiper, J. S. Gemini Surfactants. *Angew. Chem. Int. Ed.* **2000**, *39* (11), 1906–1920. [https://doi.org/10.1002/1521-3773\(20000602\)39:11<1906::AID-ANIE1906>3.0.CO;2-Q](https://doi.org/10.1002/1521-3773(20000602)39:11<1906::AID-ANIE1906>3.0.CO;2-Q).
- (8) Kelly, H. P. Many-Body Perturbation Theory Applied to Atoms. *Phys. Rev.* **1964**, *136* (3B), B896–B912. <https://doi.org/10.1103/PhysRev.136.B896>.
- (9) Menger, F. M.; Littau, C. A. Gemini-Surfactants: Synthesis and Properties. *J. Am. Chem. Soc.* **1991**, *113* (4), 1451–1452. <https://doi.org/10.1021/ja00004a077>.
- (10) Wang, X.; Wang, J.; Wang, Y.; Ye, J.; Yan, H.; Thomas, R. K. Micellization of a Series of Dissymmetric Gemini Surfactants in Aqueous Solution. *J. Phys. Chem. B* **2003**, *107* (41), 11428–11432. <https://doi.org/10.1021/jp035198z>.
- (11) Rosen, M. J.; Tracy, D. J. Gemini Surfactants. *Journal of Surfactants and Detergents* **1998**, *1* (4).
- (12) De, S.; Malik, S.; Ghosh, A.; Saha, R.; Saha, B. A Review on Natural Surfactants. *RSC Adv.* **2015**, *5* (81), 65757–65767. <https://doi.org/10.1039/C5RA11101C>.
- (13) Gruen, D. W. R. A Model for the Chains in Amphiphilic Aggregates. 1. Comparison with a Molecular Dynamics Simulation of a Bilayer. *J. Phys. Chem.* **1985**, *89* (1), 146–153. <https://doi.org/10.1021/j100247a032>.
- (14) Ramadan, M. S.; Evans, D. F.; Lumry, R. Why Micelles Form in Water and Hydrazine. A Reexamination of the Origins of Hydrophobicity. *J. Phys. Chem.* **1983**, *87* (22), 4538–4543. <https://doi.org/10.1021/j100245a040>.
- (15) Shinoda, K. “Iceberg” Formation and Solubility. *J. Phys. Chem.* **1977**, *81* (13), 1300–1302. <https://doi.org/10.1021/j100528a016>.

- (16) Maiti, P. K.; Lansac, Y.; Glaser, M. A.; Clark, N. A.; Rouault, Y. Self-Assembly in Surfactant Oligomers: A Coarse-Grained Description through Molecular Dynamics Simulations. *Langmuir* **2002**, *18* (5), 1908–1918. <https://doi.org/10.1021/la0111203>.
- (17) Poolakkandy, R. R.; Menampambath, M. M. Soft-Template-Assisted Synthesis: A Promising Approach for the Fabrication of Transition Metal Oxides. *Nanoscale Adv.* **2020**, *2* (11), 5015–5045. <https://doi.org/10.1039/D0NA00599A>.
- (18) Singer, O. M.; Campbell, J. W.; Hoare, J. G.; Masuda, J. D.; Marangoni, G.; Singer, R. D. Improved Green Synthesis and Crystal Structures of Symmetrical Cationic Gemini Surfactants. *ACS Omega* **2022**, *7* (39), 35326–35330. <https://doi.org/10.1021/acsomega.2c05073>.
- (19) Elgendy, A. A.; Clark, A. M.; Johnson, H. G.; Bahadur, P.; Singer, O. M.; Hoare, J. G.; Christie, L. D.; Singer, R. D.; Marangoni, D. G. The Thermodynamics of Micelle Formation of 10-Series Symmetric and Dissymmetric Cationic Gemini Surfactants. *J Therm Anal Calorim* **2026**. <https://doi.org/10.1007/s10973-025-15135-2>.
- (20) Tomberg, A. GAUSSIAN 09W TUTORIAL.
- (21) Manojlovic, J. The Krafft Temperature of Surfactant Solutions. *Therm sci* **2012**, *16* (suppl. 2), 631–640. <https://doi.org/10.2298/TSCI120427197M>.
- (22) Rubingh, D. N. Mixed Micelle Solutions. In *Solution Chemistry of Surfactants*; Mittal, K. L., Ed.; Springer New York: Boston, MA, 1979; pp 337–354. [https://doi.org/10.1007/978-1-4615-7880-2\\_15](https://doi.org/10.1007/978-1-4615-7880-2_15).
- (23) Clint, J. H. Micellization of Mixed Nonionic Surface Active Agents. *J. Chem. Soc., Faraday Trans. 1* **1975**, *71* (0), 1327. <https://doi.org/10.1039/f19757101327>.
- (24) Hollingsworth, S. A.; Dror, R. O. Molecular Dynamics Simulation for All. *Neuron* **2018**, *99* (6), 1129–1143. <https://doi.org/10.1016/j.neuron.2018.08.011>.
- (25) Van Der Spoel, D.; Lindahl, E.; Hess, B.; Groenhof, G.; Mark, A. E.; Berendsen, H. J. C. GROMACS: Fast, Flexible, and Free. *J Comput Chem* **2005**, *26* (16), 1701–1718. <https://doi.org/10.1002/jcc.20291>.
- (26) Berendsen, H. J. C.; Van Der Spoel, D.; Van Drunen, R. GROMACS: A Message-Passing Parallel Molecular Dynamics Implementation. *Computer Physics Communications* **1995**, *91* (1–3), 43–56. [https://doi.org/10.1016/0010-4655\(95\)00042-E](https://doi.org/10.1016/0010-4655(95)00042-E).
- (27) Lindahl, E.; Hess, B.; Van Der Spoel, D. GROMACS 3.0: A Package for Molecular Simulation and Trajectory Analysis. *J Mol Model* **2001**, *7* (8), 306–317. <https://doi.org/10.1007/s008940100045>.
- (28) Patra, M.; Karttunen, M.; Hyvönen, M. T.; Falck, E.; Lindqvist, P.; Vattulainen, I. Molecular Dynamics Simulations of Lipid Bilayers: Major Artifacts Due to Truncating Electrostatic Interactions. *Biophysical Journal* **2003**, *84* (6), 3636–3645. [https://doi.org/10.1016/S0006-3495\(03\)75094-2](https://doi.org/10.1016/S0006-3495(03)75094-2).
- (29) Pink, D. A.; Razul, M. S. G.; Gordon, T.; Quinn, B.; MacDonald, A. J. Computer Simulation Techniques for Modelling Statics and Dynamics of Nanoscale Structures. In *Edible Nanostructures*; Marangoni, A. G., Pink, D., Eds.; The Royal Society of Chemistry, 2014; p 0. <https://doi.org/10.1039/BK9781849738958-00230>.
- (30) Burrows, H. D.; Tapia, M. J.; Silva, C. L.; Pais, A. A. C. C.; Fonseca, S. M.; Pina, J.; Seixas De Melo, J.; Wang, Y.; Marques, E. F.; Knaapila, M.; Monkman, A. P.; Garamus, V. M.; Pradhan, S.; Scherf, U. Interplay of Electrostatic and Hydrophobic Effects with Binding of Cationic Gemini Surfactants and a Conjugated Polyaniion: Experimental and Molecular

- Modeling Studies. *J. Phys. Chem. B* **2007**, *111* (17), 4401–4410. <https://doi.org/10.1021/jp070100s>.
- (31) Verma, R.; Mishra, A.; Mitchell-Koch, K. R. Molecular Modeling of Cetylpyridinium Bromide, a Cationic Surfactant, in Solutions and Micelle. *J. Chem. Theory Comput.* **2015**, *11* (11), 5415–5425. <https://doi.org/10.1021/acs.jctc.5b00475>.
- (32) Goharshadi, E. K. A Review on the Radial Distribution Function: Insights into Molecular Structure, Intermolecular Interactions, and Thermodynamic Properties. *Journal of Molecular Liquids* **2025**, *433*, 127900. <https://doi.org/10.1016/j.molliq.2025.127900>.
- (33) Hernández De La Peña, L.; Kusalik, P. G. Quantum Effects in Liquid Water and Ice: Model Dependence. *The Journal of Chemical Physics* **2006**, *125* (5), 054512. <https://doi.org/10.1063/1.2238861>.
- (34) Malde, A. K.; Zuo, L.; Breeze, M.; Stroet, M.; Poger, D.; Nair, P. C.; Oostenbrink, C.; Mark, A. E. An Automated Force Field Topology Builder (ATB) and Repository: Version 1.0. *J. Chem. Theory Comput.* **2011**, *7* (12), 4026–4037. <https://doi.org/10.1021/ct200196m>.
- (35) Martínez, L.; Andrade, R.; Birgin, E. G.; Martínez, J. M. P ACKMOL : A Package for Building Initial Configurations for Molecular Dynamics Simulations. *J Comput Chem* **2009**, *30* (13), 2157–2164. <https://doi.org/10.1002/jcc.21224>.
- (36) Lebecque, S.; Crowet, J. M.; Nasir, M. N.; Deleu, M.; Lins, L. Molecular Dynamics Study of Micelles Properties According to Their Size. *Journal of Molecular Graphics and Modelling* **2017**, *72*, 6–15. <https://doi.org/10.1016/j.jm gm.2016.12.007>.
- (37) Abel, S.; Dupradeau, F.-Y.; Marchi, M. Molecular Dynamics Simulations of a Characteristic DPC Micelle in Water. *J. Chem. Theory Comput.* **2012**, *8* (11), 4610–4623. <https://doi.org/10.1021/ct3003207>.
- (38) Berendsen, H. J. C.; Grigera, J. R.; Straatsma, T. P. The Missing Term in Effective Pair Potentials. *J. Phys. Chem.* **1987**, *91* (24), 6269–6271. <https://doi.org/10.1021/j100308a038>.
- (39) Zhu, J.; Zhu, P.; Wan, Z.; Ye, Y.; Yang, K.; Kamal, S.; Tan, Y.; Rojas, O. J.; Jiang, F. Hydration-Driven Surface Engineering of Nanocellulose Films for Iridescent Structural Colors. *ACS Sustainable Chem. Eng.* **2025**, *13* (35), 14551–14560. <https://doi.org/10.1021/acssuschemeng.5c05707>.
- (40) Darden, T.; Darrin York; Pedersen, L. Particle Mesh Ewald: An  $N \cdot \log(N)$  Method for Ewald Sums in Large Systems. *The Journal of Chemical Physics* **1993**, *98* (12), 10089–10092. <https://doi.org/10.1063/1.464397>.
- (41) Overhauser, A. W. Polarization of Nuclei in Metals. *Phys. Rev.* **1953**, *92* (2), 411–415. <https://doi.org/10.1103/PhysRev.92.411>.
- (42) Charland, J. P.; Phan Viet Minh Tan; St-Jacques, M.; Beauchamp, A. L. Multinuclear NMR Study of the Disproportionation and Syn/Anti Isomerism in Solutions of Amino-Substituted Methylmercury Derivatives of Adenine and 9-Methyladenine. *J. Am. Chem. Soc.* **1985**, *107* (26), 8202–8211. <https://doi.org/10.1021/ja00312a065>.
- (43) Reyes-López, E.; Quiroz-García, B.; Carpio-Martínez, P.; Jiménez-Barbero, J.; Esturau-Escofet, N.; Cuevas, G. The Folded Conformation of Perezone Revisited. Long Range nOe Interaction in Small Molecules: Interpretable Small Signals or Useless Large Artifacts? *J. Mex. Chem. Soc.* **2017**, *61* (3). <https://doi.org/10.29356/jmcs.v61i3.343>.
- (44) M. J.Frisch, G. W.Trucks, H. B.Schlegel, G. E.Scuseria, M. A.Robb, J. R.Cheeseman, P.Hratchian, A. F.Izmaylov, J.Bloino, G.Zheng, J. L.Sonnenberg, M.Hada, M.Ehara, K.Toyota, R.Fukuda, J.Hasegawa, M.Ishida, T.Nakajima, Y.Honda, O.Kitao, H.Nakai,

- T.Vreven, J. A.Montgomery Jr., J. E.Peralta, F.Ogliaro, M.Bearpark, J. J.Heyd, E.Brothers, K. N.Kudin, V. N.Staroverov, T.Keith, R.Kobayashi, J.Normand, K.Raghavachari, A.Rendell, J. C.Burant, S. S.Iyengar, J.Tomasi, M.Cossi, N.Regga, J. M.Millam, M.Klene, J. E.Knox, J. B.Cross, V.Bakken, C.Adamo, J.Jaramillo, R.Gomperts, R. E.Stratmann, O.Yazyev, A. J.Austin, R.Cammi, C.Pomelli, J. W.Ochterski, R. L.Martin, K.Morokuma, V. G.Zakrzewski, G. A.Voth, P.Salvador, J. J.Dannenberg, S.Dapprich, A. D.Daniels, Wallingford, CT, 2013.
- (45) Becke, Axel D. "DFT studies on the pairing abilities of the one-electron reduced or oxidized adenine–thymine base pair." *Chemical Physics* 98.7 (1993): 5648-5652.
- (46) van Os, Nico M., Jan Remees Haak, and Leonardus Antonius Maria Rupert. *Physico-chemical properties of selected anionic, cationic and nonionic surfactants*. Elsevier, 2012.
- Myers, D., *Surfaces, Interfaces, and Colloids*, John Wiley and Sons, New York, USA, 1999
- (47) ChemSketch, version 2022.1.2, Advanced Chemistry Development, Inc. (ACD/Labs), Toronto, ON, Canada, [www.acdlabs.com](http://www.acdlabs.com).
- (48) Rassolov, Vitaly A., et al. "6-31G\* basis set for atoms K through Zn." *The Journal of chemical physics* 109.4 (1998): 1223-1229.
- (49) *Surfactants market size, share, trends, Global Report, 2034*. Surfactants Market Size, Share, Trends, Global Report, 2034. (n.d.-a).  
<https://www.fortunebusinessinsights.com/surfactants-market-102385#:~:text=The%20global%20surfactants%20market%20size,efficient%20and%20eco%2Dfriendly%20products>.
- (50) Maiti, P.K. and Chowdhury, D., *J. Chem. Phys.*, 1998, 109, 5126-513.
- (51) MacNeil, N.; Elgendy A.; Wettig, S.; Christie, L.; Singer, R.; Marangoni D.G. Micellar Packing of Dimeric Surfactants. *Canadian journal of chemistry*. Accepted for publication.